

**Elemental analysis results for air particulate matter
collected in Auckland, 2006–2021**

PK Davy

WJ Trompetter

**GNS Science Consultancy Report 2021/45
November 2021**



DISCLAIMER

This report has been prepared by the Institute of Geological and Nuclear Sciences Limited (GNS Science) exclusively for and under contract to Auckland Council. Unless otherwise agreed in writing by GNS Science, GNS Science accepts no responsibility for any use of or reliance on any contents of this report by any person other than Auckland Council and shall not be liable to any person other than Auckland Council, on any ground, for any loss, damage or expense arising from such use or reliance.

Use of Data:

Date that GNS Science can use associated data: June 2021

BIBLIOGRAPHIC REFERENCE

Davy PK, Trompetter WJ. 2021. Elemental analysis results for air particulate matter collected in Auckland, 2006–2021. Lower Hutt (NZ): GNS Science. 57 p. Consultancy Report 2021/45.

CONTENTS

EXECUTIVE SUMMARY	IV
1.0 INTRODUCTION	1
2.0 METHODOLOGY	2
2.1 Location of Auckland Particulate Matter Speciation Monitoring Sites	2
2.2 Sample Collection and Elemental Analysis of Particulate Matter	3
2.3 Comparison of Continuous PM ₁₀ Mass Measurement with Gravimetric Data ...	3
3.0 PAN-AUCKLAND BLACK CARBON AND ELEMENTAL CONCENTRATIONS: TEMPORAL PATTERNS AND TRENDS IN PARTICULATE MATTER COMPOSITION (2006–2021)	5
4.0 WESTLAKE GIRLS HIGH SCHOOL, TAKAPUNA	14
4.1 Site Description	14
4.2 Air Particulate Matter Samples and Monitoring Period	14
4.2.1 Elemental Analysis of PM _{2.5} Samples from the Takapuna Site.....	15
4.2.2 Elemental Analysis of PM ₁₀ Samples from the Takapuna Site	17
5.0 QUEEN STREET, CENTRAL AUCKLAND	19
5.1 Site Description	19
5.2 Air Particulate Matter Samples and Monitoring Period	19
5.2.1 Elemental Analysis of PM _{2.5} Samples from the Queen Street Site	20
5.2.2 Elemental Analysis of PM ₁₀ Samples from the Queen Street Site	22
6.0 KYBER PASS ROAD, NEWMARKET	24
6.1 Site Description	24
6.2 Air Particulate Matter Samples and Monitoring Period	24
6.2.1 Elemental Analysis of PM _{2.5} Samples from the Khyber Pass Road Site	25
6.2.2 Elemental Analysis of PM ₁₀ Samples from the Khyber Pass Road Site	27
7.0 GAVIN STREET, PENROSE	29
7.1 Site Description	29
7.2 Air Particulate Matter Samples and Monitoring Period	29
7.2.1 Elemental Analysis of PM _{2.5} Samples from the Penrose Site	30
7.2.2 Elemental Analysis of PM ₁₀ Samples from the Penrose Site.....	32
7.2.3 Elemental Analysis of Partisol PM ₁₀ Samples from the Penrose Site.....	34
8.0 LINCOLN ROAD, HENDERSON	36
8.1 Site Description	36
8.2 Air Particulate Matter Samples and Monitoring Period	36
8.2.1 Elemental Analysis of PM ₁₀ Samples from the Henderson Site.....	37
8.3 Re-Analysis of Henderson Filters by X-Ray Fluorescence Spectroscopy.....	38
9.0 REFERENCES	42

FIGURES

Figure 2.1	Location of the three monitoring sites currently included in the Auckland particulate matter speciation network.....	2
Figure 2.2	Comparison between continuous PM ₁₀ mass concentrations and gravimetric mass measurements (24-hour averages) for Henderson and Takapuna (2006–2017).....	3
Figure 2.3	Comparison between continuous instrumental PM ₁₀ mass concentrations and gravimetric mass measurements (24-hour averages) for Henderson, Takapuna and Queen Street.....	4
Figure 3.1	Box and whisker plot for pan-Auckland PM _{2.5} elemental concentrations.....	5
Figure 3.2	Box and whisker plot for pan-Auckland PM ₁₀ elemental concentrations.....	5
Figure 3.3	Trend analysis for pan-Auckland PM _{2.5} concentrations.....	6
Figure 3.4	Trend analysis for key pan-Auckland PM _{2.5} elemental concentrations.....	6
Figure 3.5	Temporal variation analysis for pan-Auckland PM _{2.5} concentrations and key PM _{2.5} elemental components.....	8
Figure 3.6	Trend analysis (2006–2021) for pan-Auckland PM ₁₀ concentrations.....	9
Figure 3.7	Trend analysis for key pan-Auckland PM ₁₀ elemental concentrations.....	10
Figure 3.8	Trend analysis for PM ₁₀ hydrogen elemental concentrations at the three current Auckland Council speciation monitoring sites.....	12
Figure 3.9	Temporal variation analysis for pan-Auckland PM ₁₀ concentrations and key PM ₁₀ elemental components.....	13
Figure 4.1	Aerial image showing location of Takapuna monitoring site.....	14
Figure 4.2	Correlation plot for key PM _{2.5} elemental components at the Takapuna site.....	16
Figure 4.3	Correlation plot for key PM ₁₀ elemental components at the Takapuna site.....	18
Figure 5.1	Aerial image showing location of Queen Street monitoring site.....	19
Figure 5.2	Correlation plot for key PM _{2.5} elemental components at the Queen Street site.....	21
Figure 5.3	Correlation plot for key PM ₁₀ elemental components at the Queen Street site.....	23
Figure 6.1	Aerial image showing location of Khyber Pass Road monitoring site.....	24
Figure 6.2	Correlation plot for key PM _{2.5} elemental components at the Khyber Pass Road site.....	26
Figure 6.3	Correlation plot for key PM ₁₀ elemental components at the Khyber Pass Road site.....	28
Figure 7.1	Aerial image showing location of Penrose monitoring site.....	29
Figure 7.2	Correlation plot for key PM _{2.5} elemental components at the Penrose site.....	31
Figure 7.3	Correlation plot for key PM ₁₀ elemental components at the Penrose site.....	33
Figure 7.4	Correlation plot for key Partisol PM ₁₀ elemental components at the Penrose site.....	35
Figure 8.1	Aerial view showing location of Henderson monitoring site.....	36
Figure 8.2	Correlation plot for key PM ₁₀ elemental components at the Henderson site.....	38
Figure 8.3	Monthly average arsenic and lead concentrations in PM ₁₀ at the Henderson air quality monitoring site.....	40
Figure 8.4	Annual average arsenic concentrations at Henderson.....	40
Figure 8.5	Trend analysis for arsenic concentrations at Henderson.....	41
Figure 8.6	Trend analysis for lead concentrations at Henderson.....	41

TABLES

Table 2.1	Auckland monitoring site summary: size fraction, sample number and sample period.....	2
Table 4.1	Elemental analysis results for PM _{2.5} at the Takapuna site	15
Table 4.2	Elemental analysis results for PM ₁₀ at the Takapuna site	17
Table 5.1	Elemental analysis results for PM _{2.5} at the Queen Street site.....	20
Table 5.2	Elemental analysis results for PM ₁₀ at the Queen Street site	22
Table 6.1	Elemental analysis results for PM _{2.5} at the Khyber Pass Road site	25
Table 6.2	Elemental analysis results for PM ₁₀ at the Khyber Pass Road site.....	27
Table 7.1	Elemental analysis results for PM _{2.5} at the Penrose site.....	30
Table 7.2	Elemental analysis results for PM ₁₀ at the Penrose site	32
Table 7.3	Elemental analysis results for PM ₁₀ at the Penrose site	34
Table 8.1	Elemental analysis results for PM ₁₀ at the Henderson site.....	37
Table 8.2	Elemental concentrations by XRF in PM ₁₀ samples from the Henderson site	39

APPENDICES

APPENDIX 1	SAMPLE ANALYSIS AND DATA QUALITY ASSURANCE.....	47
A1.1	Black Carbon Analysis.....	47
A1.2	Elemental Concentrations by Ion Beam Analysis.....	48
	A1.2.1 Particle-Induced X-Ray Emission.....	49
	A1.2.2 Particle-Induced Gamma-Ray Emission	50
A1.3	Elemental Concentrations by X-Ray Fluorescence Spectroscopy.....	51
A1.4	X-Ray Fluorescence Spectroscopy and Ion Beam Analysis Data Reporting ..	52
	A1.4.1 Limits of Detection and Uncertainty Reporting for Elements	52
A1.5	Dataset Quality Assurance	54
	A1.5.1 Mass Reconstruction and Mass Closure.....	54

APPENDIX FIGURES

Figure A1.1	Particulate matter analysis chamber with its associated detectors.....	48
Figure A1.2	Schematic of the typical ion beam analysis experimental set-up at GNS Science.	49
Figure A1.3	Typical particle-induced X-ray emission spectrum for an aerosol sample.	49
Figure A1.4	Typical particle-induced gamma-ray emission spectrum for an aerosol sample.....	50
Figure A1.5	The PANalytical Epsilon 5 spectrometer.	51
Figure A1.6	Example X-ray spectrum from a PM ₁₀ sample.....	52
Figure A1.7	Elemental limits of detection for particle-induced X-ray emission routinely achieved at the GNS Science Ion Beam Analysis facility for air filters.....	54
Figure A1.8	Plot of elemental mass reconstruction against gravimetric for Takapuna PM ₁₀ mass.	56
Figure A1.9	Plot of elemental mass reconstruction against gravimetric for Takapuna PM ₁₀ mass.	56
Figure A1.10	Plot of elemental mass reconstruction against gravimetric for Henderson PM ₁₀ mass.....	57

EXECUTIVE SUMMARY

This report contains summary results and statistics for the elemental analysis of a total of 14,700 filter-based PM_{2.5} and PM₁₀ air particulate matter samples collected as part of an Auckland Council environmental monitoring programme. The samples were collected over a 14-year period from December 2005 to January 2021 at five air quality monitoring sites located in Auckland City.

The particulate matter samples have been analysed for a range of 30 elements and black carbon. The elemental data shows the significant impact that anthropogenic activities have on particulate matter concentrations. Long-term trends in elemental concentrations vary across the measurement suite and are likely to be dependent on the activity and emissions of particulate matter from contributing sources.

Detailed analyses of sources contributing to Auckland particulate matter concentrations derived from the elemental analysis were provided in a report: *Composition, sources and long-term trends for Auckland air particulate matter* (Davy and Trompetter 2020; GNS Science Consultancy Report 2019/151) for the period 2006–2019, which explains the observed spatial and temporal trends for the sources of elemental concentrations at each sampling location.

1.0 INTRODUCTION

Sampling of particulate matter for elemental compositional analysis began at the Auckland monitoring sites in December 2005. This report presents an annual summary of the elemental analysis results from the Auckland speciation sites to January 2021. The report primarily provides an overview of the collection sites, particulate matter measurement methods and long-term trends in elemental concentrations of this dataset. A description of the ion beam analysis (IBA) and X-ray fluorescence (XRF) methods for determining the elemental concentrations is presented in the Appendices. Detailed analyses of the sources contributing to Auckland particulate matter concentrations derived from the elemental analysis were provided in a previous report: *Composition, sources and long-term trends for Auckland air particulate matter* (Davy and Trompetter 2020; GNS Science Consultancy Report 2019/151) for the period 2006–2019, which explains the observed spatial and temporal trends in the sources of elemental concentrations for each sampling location.

2.0 METHODOLOGY

2.1 Location of Auckland Particulate Matter Speciation Monitoring Sites

Sampling of particulate matter for elemental speciation began at the monitoring sites in December 2005. This report presents the elemental analysis results from Auckland speciation sites to the beginning of 2021. Sampling at a number of sites was discontinued during 2015 (Khyber Pass Road PM_{2.5} and PM₁₀, Queen Street PM_{2.5}) and June 2016 (Takapuna PM_{2.5}, and Penrose PM_{2.5} and PM₁₀ speciation monitoring), as indicated in Table 2.1. Figure 2.1 presents the locations of each of the monitoring sites described in this data summary.



Figure 2.1 Location of the three monitoring sites (●) currently included in the Auckland particulate matter speciation network (source: Google Earth).

Table 2.1 presents a summary of the size fractions and number of samples from each of the monitoring sites.

Table 2.1 Auckland monitoring site summary: size fraction, sample number and sample period.

Site	PM Size Fraction	Instrument Type	Number of Filter Samples	Sample Period
Takapuna	PM ₁₀	Partisol 2000	1448	December 2005 – January 2021
Queen Street	PM ₁₀	Partisol 2000	3613	December 2005 – January 2021
Henderson	PM ₁₀	Partisol 2000	1385	August 2006 – January 2021

2.2 Sample Collection and Elemental Analysis of Particulate Matter

Samples of PM collected on filters from five Auckland Council air quality monitoring sites were received by GNS Science on an annual basis. Elemental concentrations in the particle samples were determined by IBA techniques at the New Zealand IBA facility at Gracefield, Lower Hutt. A full description of the IBA methods and data analysis techniques used in this report is provided in Appendix 1. In addition, all PM₁₀ filter samples from Henderson have also been analysed by XRF spectroscopy that provides complimentary multi-elemental concentrations, but with greater sensitivity for heavy metals. The XRF data for Henderson is provided alongside the IBA data, and a description of the XRF spectroscopic technique is also given in Appendix 1.

All particulate matter sampling, filter weighing and systems maintenance at sampling sites from 2006 until June 2017 was carried out by Watercare Services Limited (WSL) on behalf of the Auckland Council. As such, WSL maintains all records of equipment, flow rates, filter weighing and sampling methodologies used for the particulate matter sampling regimes. From July 2017, all particulate matter sampling and systems maintenance at sampling sites was carried out by Mote Limited (ML) on behalf of the Auckland Council. Therefore, ML now maintains all records of equipment, flow rates and sampling methodologies used for the particulate matter sampling regimes.

2.3 Comparison of Continuous PM₁₀ Mass Measurement with Gravimetric Data

Following the re-organisation of sampling and change in air quality monitoring service provider, it was decided that use of continuous mass concentration data (e.g. from a beta attenuation monitor [BAM]) was sufficient for the speciation and source apportionment analyses. Figure 2.2 presents a plot for gravimetric mass and continuous PM₁₀ mass measurements for the Henderson and Takapuna monitoring sites (2006–2017). While some scatter is evident, the two measures of PM₁₀ mass provide equivalent results for the purposes of receptor modelling. In addition, this approach saves time and costs for each individual filter to be pre- and post-weighed.

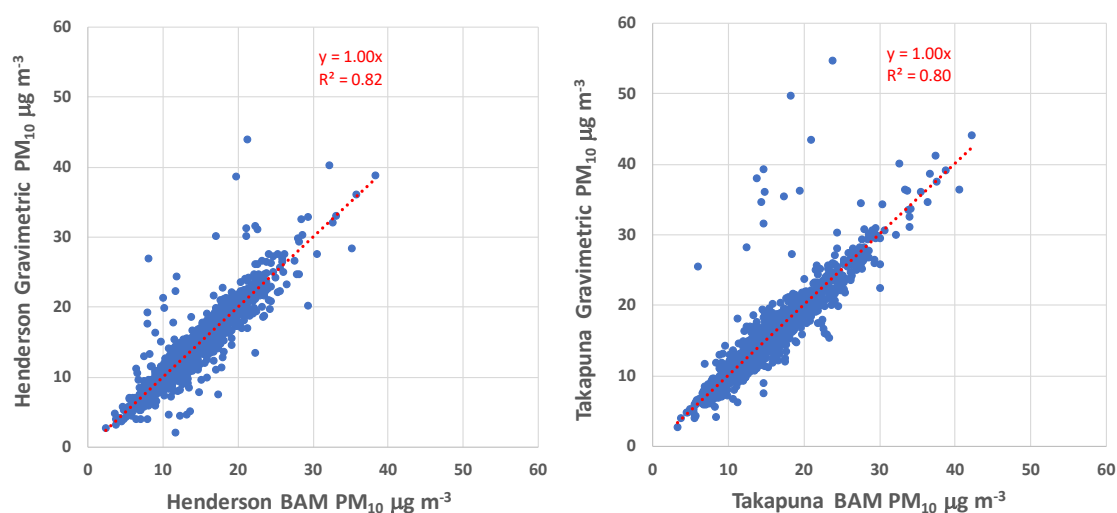


Figure 2.2 Comparison between continuous PM₁₀ (beta attenuation monitor [BAM]) mass concentrations and gravimetric mass measurements (24-hour averages) for Henderson and Takapuna (2006–2017).

As part of the ongoing quality assurance for the speciation datasets, a set of 10 gravimetric filter analyses was taken for each monitoring site during December 2018, March 2020 and July 2020 to compare with the instrumental mass concentration data. Figure 2.3 presents the comparison between instrumental and gravimetric PM₁₀ mass concentrations for the three currently operating Auckland PM₁₀ speciation sites (Henderson, Takapuna and Queen Street). Note that the Henderson and Takapuna sites operate BAMs as the instrumental PM₁₀ mass concentration monitor, while a Teledyne T640 (optical scattering) system is used at the Queen Street site.

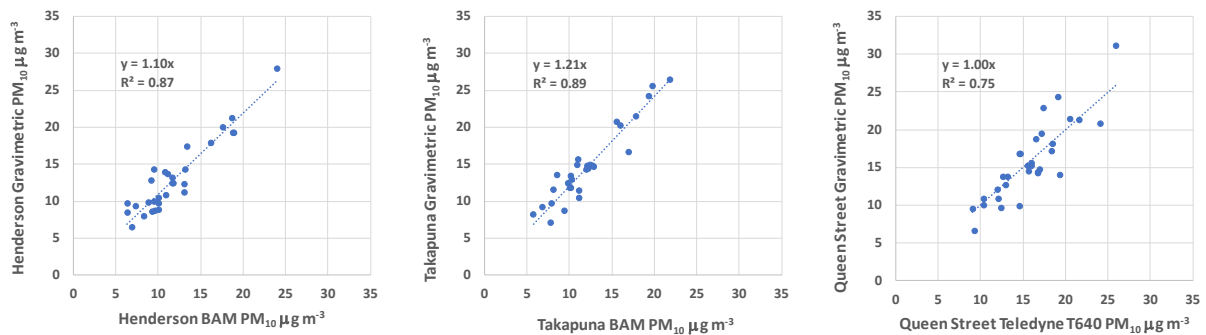


Figure 2.3 Comparison between continuous instrumental PM₁₀ mass concentrations and gravimetric mass measurements (24-hour averages) for Henderson, Takapuna and Queen Street (December 2018, March 2020 and July 2020).

3.0 PAN-AUCKLAND BLACK CARBON AND ELEMENTAL CONCENTRATIONS: TEMPORAL PATTERNS AND TRENDS IN PARTICULATE MATTER COMPOSITION (2006–2021)

The multi-site particulate matter speciation data provides the opportunity to aggregate the data from all sites and examine the concentration trends for individual elemental species. This is of interest in terms of the overall environmental loadings originating from air particulate matter emissions. Figure 3.1 presents a box and whisker plot for key elemental concentrations in PM_{2.5}, and Figure 3.2 presents the PM₁₀ elemental data. Note that the top and bottom of the box are the upper and lower concentration quartiles, the line dividing the box is the median and the blue dot is the mean, while the whiskers show the 5th and 95th percentile concentrations.

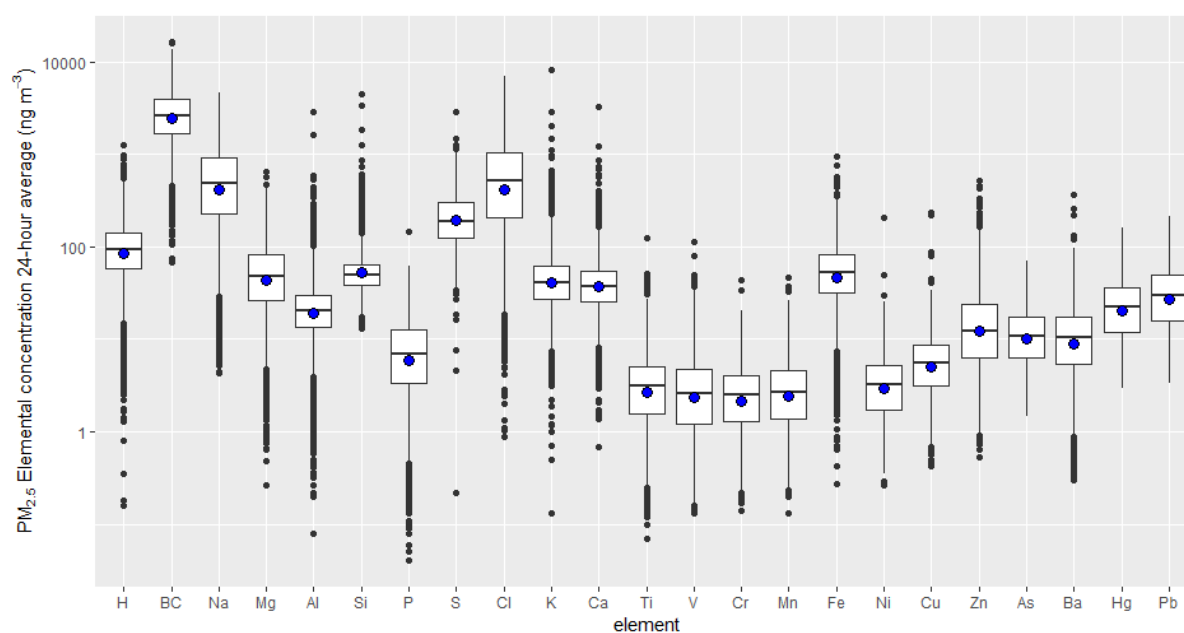


Figure 3.1 Box and whisker plot for pan-Auckland PM_{2.5} elemental concentrations.

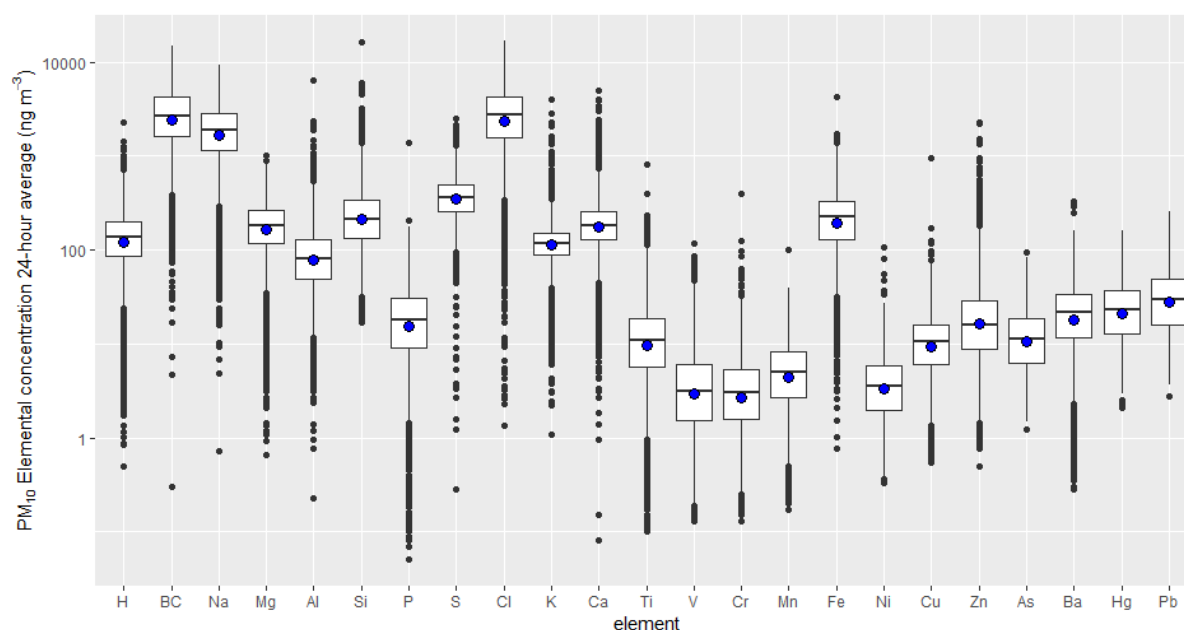


Figure 3.2 Box and whisker plot for pan-Auckland PM₁₀ elemental concentrations.

The trend analysis of pan-Auckland PM_{2.5} shows that concentrations have been decreasing (statistically significant at 99.9% confidence intervals) over the monitoring period and that this decrease has been consistent across the seasons, as shown in Figure 3.3.

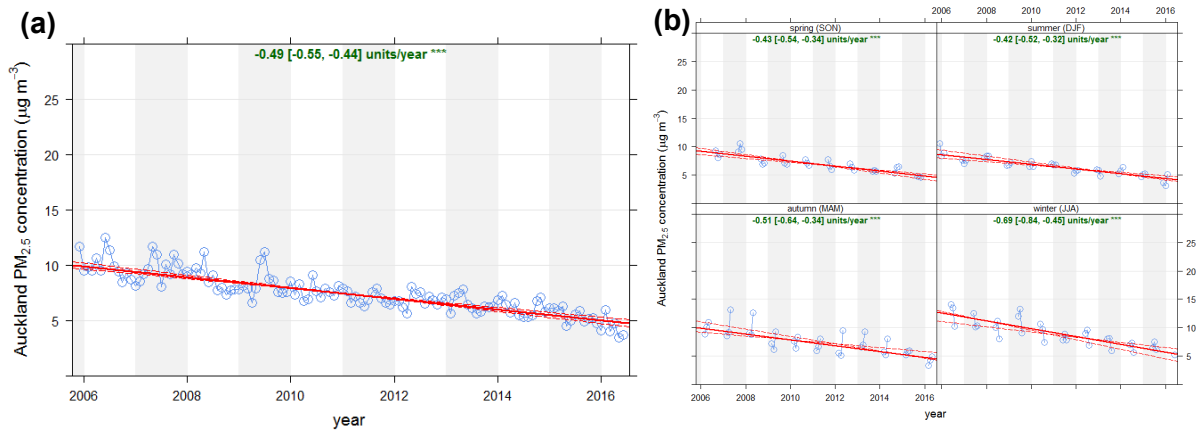


Figure 3.3 Trend analysis for pan-Auckland PM_{2.5} concentrations; (a) de-seasonalised and (b) seasonal trends.

Figure 3.4 presents the trends for key elemental component PM_{2.5} species. As would be expected with the decreasing PM_{2.5} concentrations, most of the elemental components also show statistically significant decreasing concentration trends, except for hydrogen (statistically significant increase) and zinc (no trend evident), and these will be linked to the trends in activity for emission sources of these elements.

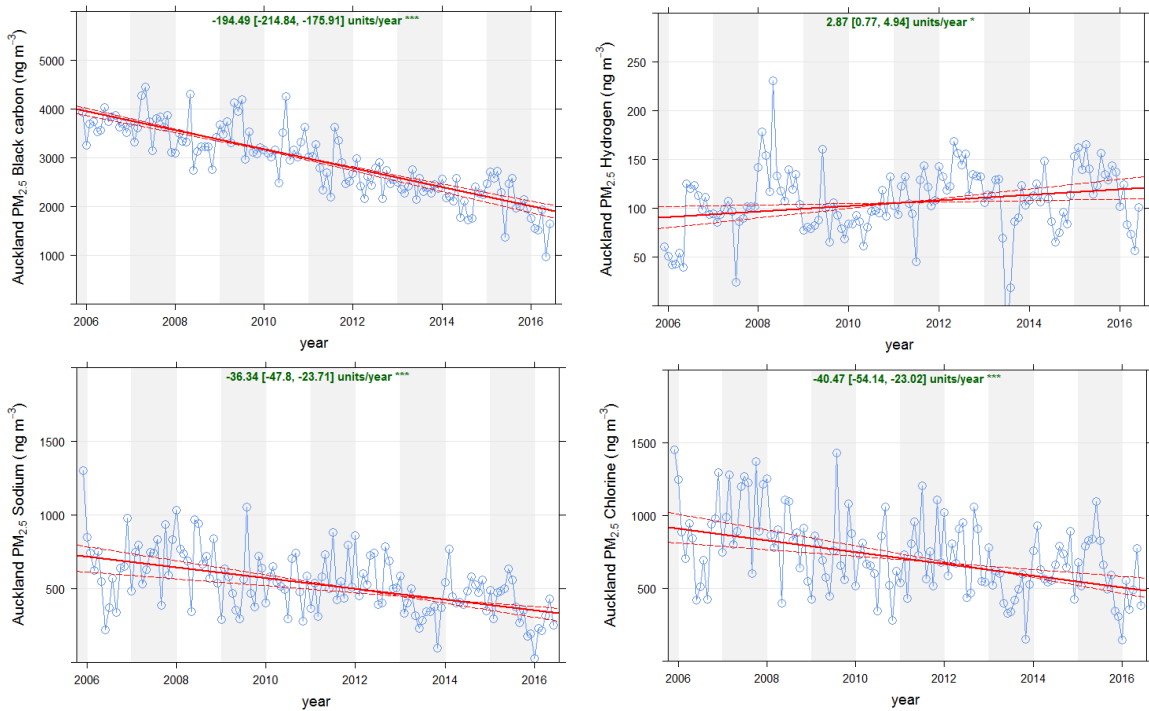


Figure 3.4 Trend analysis for key pan-Auckland PM_{2.5} elemental concentrations. Continued over the page.

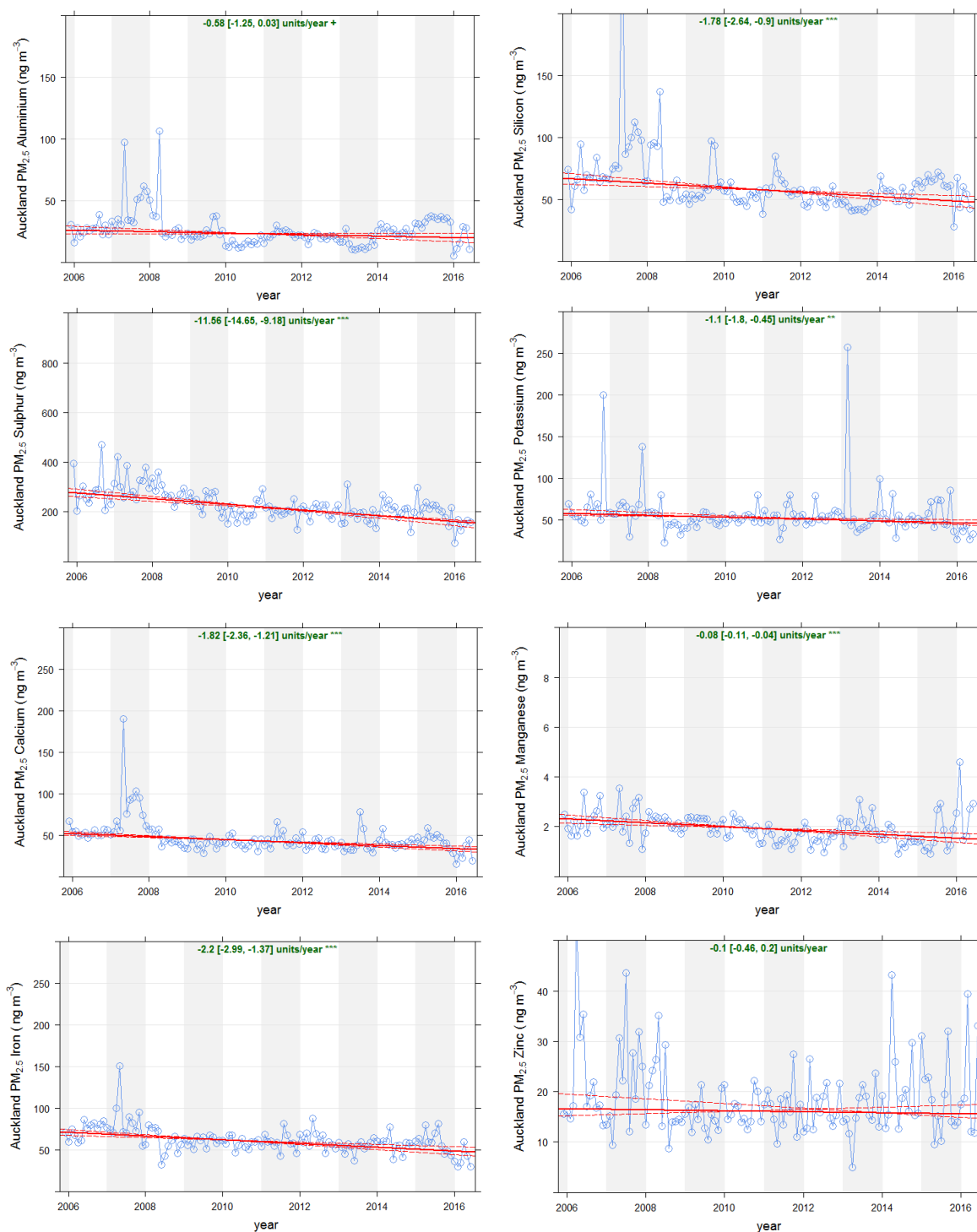


Figure 3.4 Continued. Trend analysis for key pan-Auckland PM_{2.5} elemental concentrations.

Temporal variations in concentrations examined for key pan-Auckland elemental species (Figure 3.5) show that PM_{2.5} and all elemental species, except for chlorine and sulphur, have a weekday-weekend concentration differential, indicating that the dominant emission source is likely to be anthropogenic. Any purely natural source would present a random concentration pattern without preference for particular days of the week. Sulphur is likely to be influenced by natural (oceanic biota, volcanic emissions) and anthropogenic (combustion of sulphur containing fuels) sources, while chlorine concentrations are largely due to natural marine aerosol (sea salt).

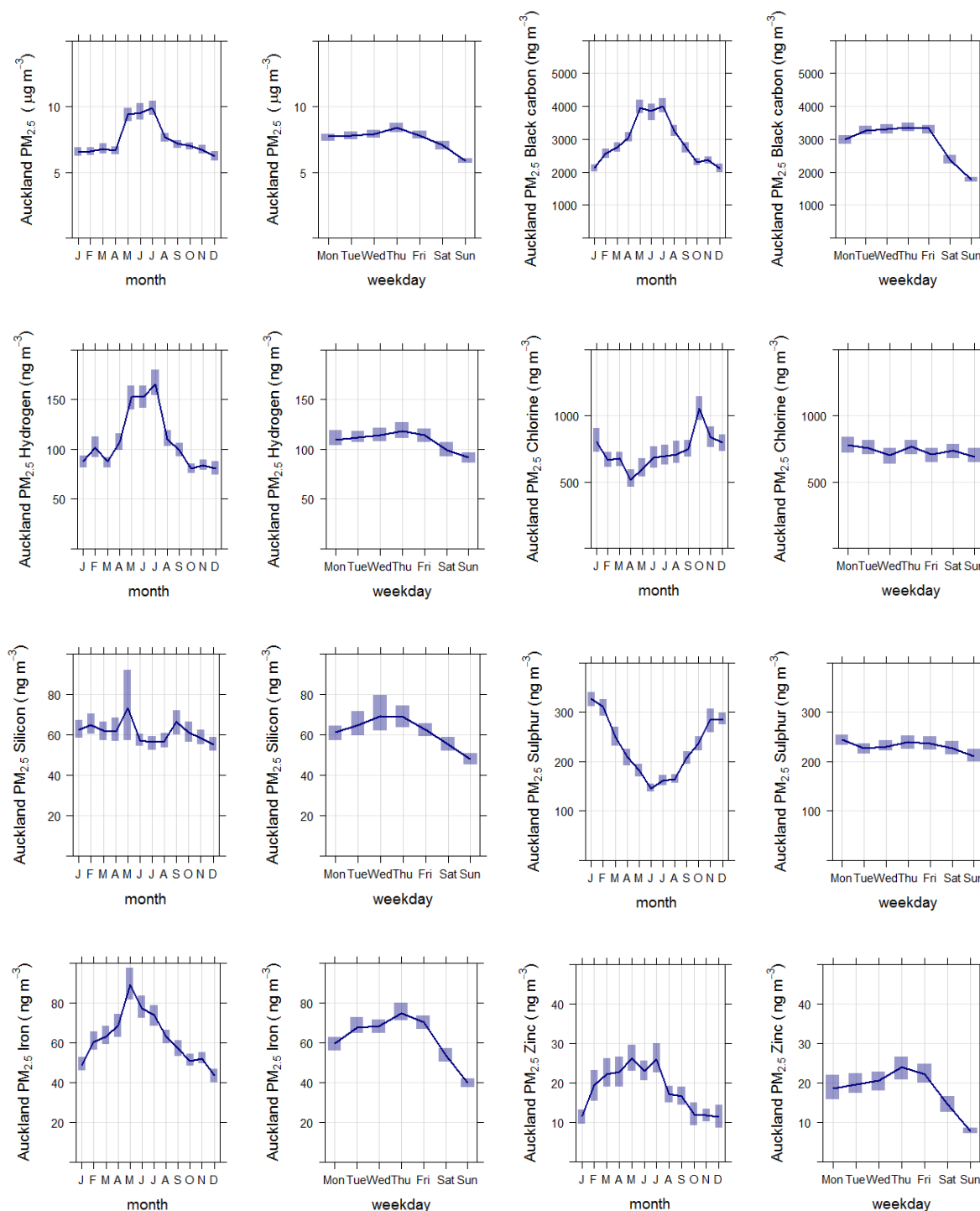


Figure 3.5 Temporal variation analysis for pan-Auckland PM_{2.5} concentrations and key PM_{2.5} elemental components.

Similar to the case of PM_{2.5}, the long-term trends (2006–2021) for pan-Auckland PM₁₀ (i.e. a combination of data from Henderson, Takapuna and Queen Street speciation monitoring sites) shows that concentrations have been decreasing (statistically significant at 99.9% confidence intervals) over the monitoring period and that this decrease has been consistent across the seasons, as shown in Figure 3.6. The critical relationship between PM_{2.5} and PM₁₀ is that the decreasing concentration trend observed for PM₁₀ (up until June 2016, when the PM_{2.5} speciation dataset ends) was due to the decrease in PM_{2.5} concentrations.

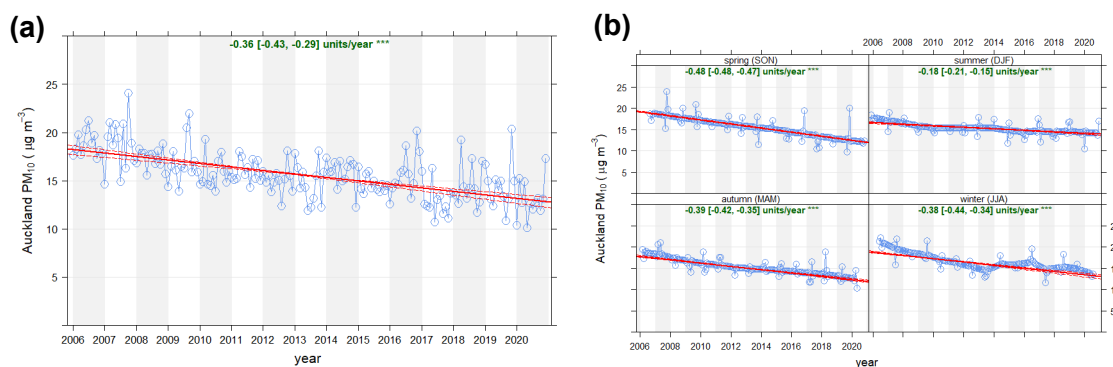


Figure 3.6 Trend analysis (2006–2021) for pan-Auckland PM₁₀ concentrations; (a) de-seasonalised and (b) seasonal trends. All trends were significant to the 99.9% confidence intervals.

Figure 3.7 presents the long-term trends (2006–2021) for key elemental component PM₁₀ species. Similar patterns were observed for PM₁₀ composition as with the decreasing PM_{2.5} concentrations. Most of the elemental components also show statistically significant (at the 99.9% confidence interval) decreasing concentration trends, except for hydrogen (statistically significant increase at the 99.9% confidence interval) and potassium (no trend evident), and these will be linked to the source emission trends for these elements. It is interesting to note that the impacts of the COVID-19 lockdowns do not necessarily stand out in the long-term data but were shown to have a short-term impact, particularly for motor-vehicle-related black carbon (BC) emissions (Patel et al. 2020).

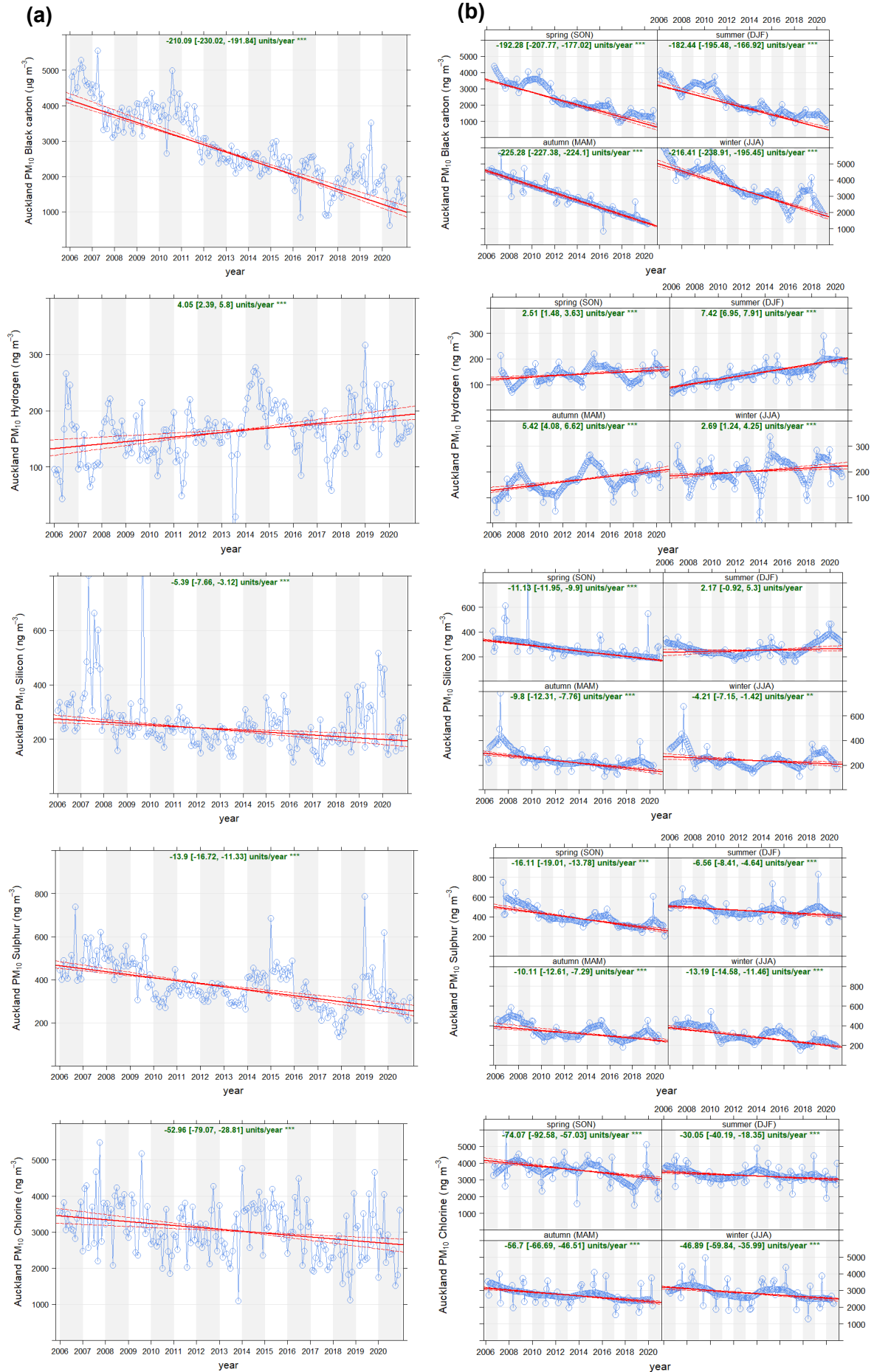


Figure 3.7 Trend analysis for key pan-Auckland PM₁₀ elemental concentrations. Continued over the page.

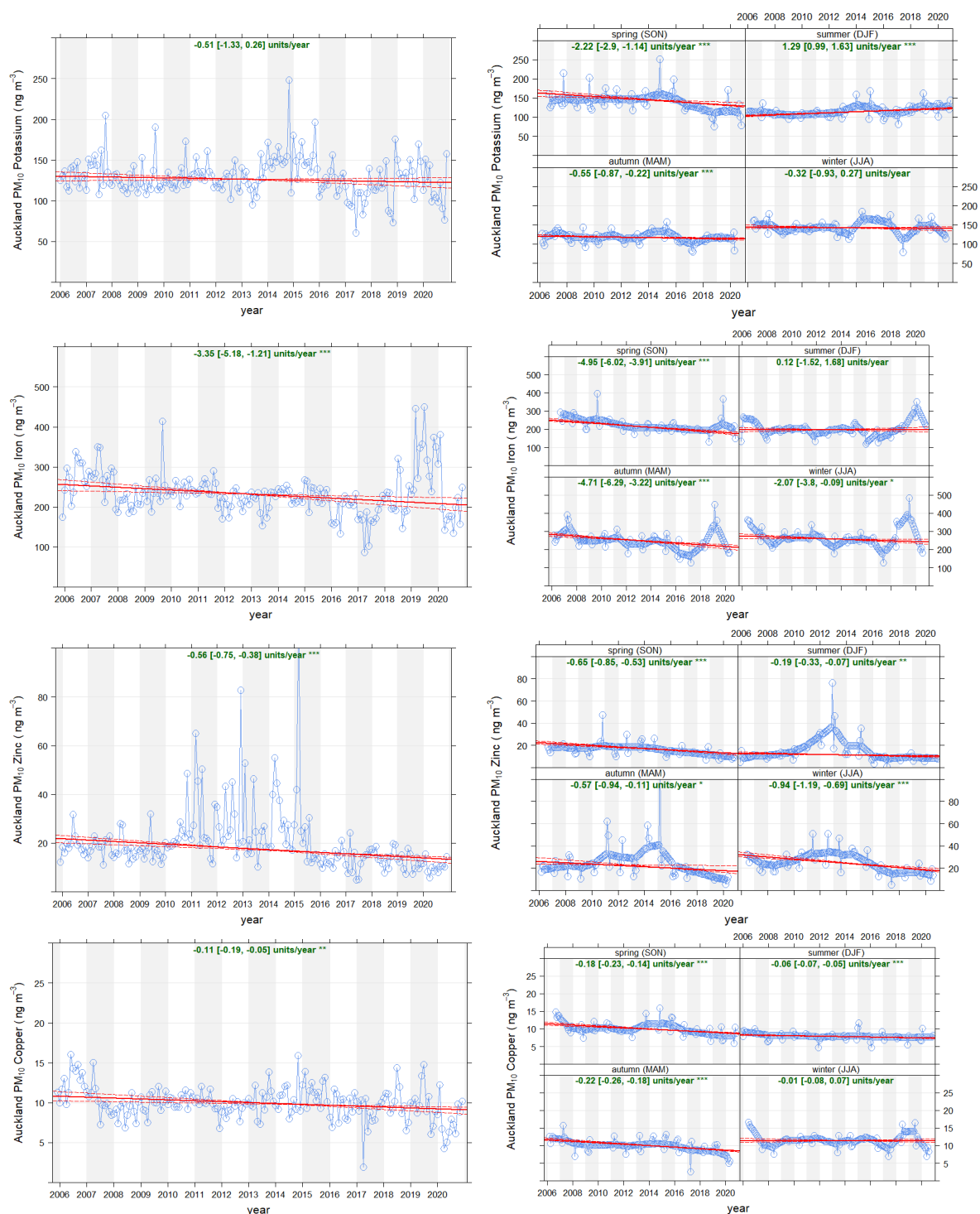


Figure 3.7 Continued. Trend analysis for key pan-Auckland PM₁₀ elemental concentrations; (a) de-seasonalised and (b) seasonal trends.

The year-on-year increasing trend for pan-Auckland hydrogen concentrations is interesting, as it is evident that the greatest increase was during summer. There are several key sources of airborne particulate matter hydrogen:

- Hydrocarbon compounds from incomplete combustion of fuels (motor vehicle or biomass combustion).
- Secondary organic aerosol (SOA) from volatile organic precursors, which can either be anthropogenic (solvents/fuel vapours) or biogenic (oceanic biota or terrestrial tree) emissions.

- Ammonia species, most likely as ammonium sulphate (i.e. secondary sulphate) or ammonium nitrate.
- Perhaps more minor sources of particulate matter hydrogen are those species bound as part of mineral structures.

Figure 3.8 presents the long-term trends in PM₁₀ hydrogen concentrations at Henderson, Takapuna and Queen Street, respectively.

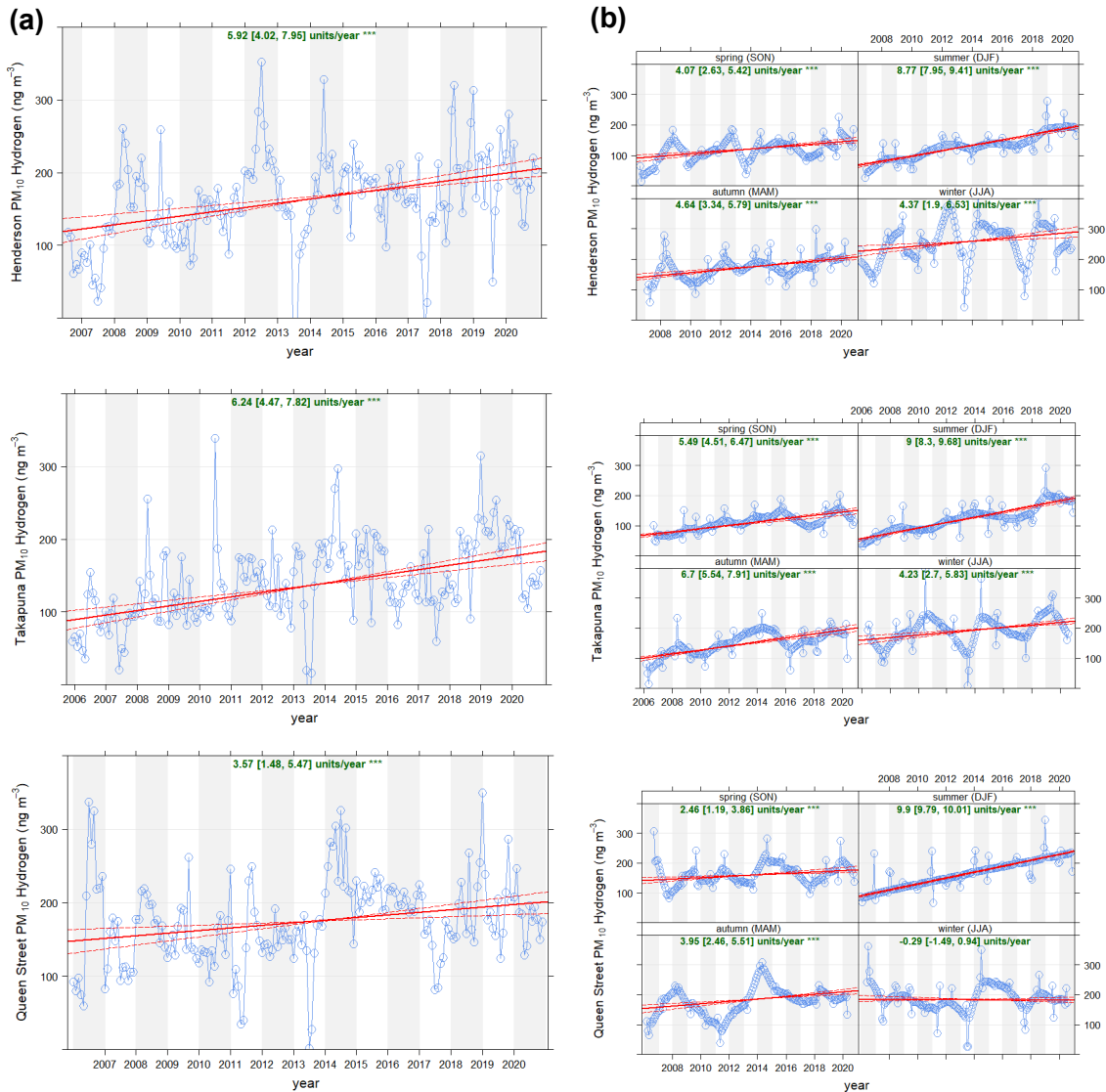


Figure 3.8 Trend analysis for PM₁₀ hydrogen elemental concentrations at the three current Auckland Council speciation monitoring sites; (a) de-seasonalised and (b) seasonal trends.

Figure 3.8 shows that all sites had a statistically significant (99.9 percentile confidence intervals) increasing trend in concentration for hydrogen. On a seasonal basis, all sites had statistically significant increasing trends, except for the winter period at the Queen Street site where no trend was observed (i.e. concentrations were static over the 14-year monitoring period). Again, it is evident that the greatest increase was during summer, with all sites experiencing similar rates (approximately 9 ng/m³/year). This indicates that a regional source was likely to be responsible for driving this increase, although exactly what that source may be is unclear at this stage. The summer increase suggests that it may be a secondary aerosol source such as SOA, but this would need to be explored further to confirm the processes that give rise to such trends.

The temporal variation in concentrations were examined for key pan-Auckland elemental species (Figure 3.9) and shows that PM₁₀ and key species (H, BC, Si, Fe, Zn), except for chlorine and sulphur, have a weekday-weekend concentration differential, indicating that the dominant emission source is likely to be anthropogenic. Any purely natural source would present a random concentration pattern without preference for particular days of the week. Sulphur is likely to be influenced by natural (oceanic biota, volcanic emissions) and anthropogenic (combustion of sulphur containing fuels) sources, while chlorine concentrations are largely due to natural marine aerosol (sea salt).

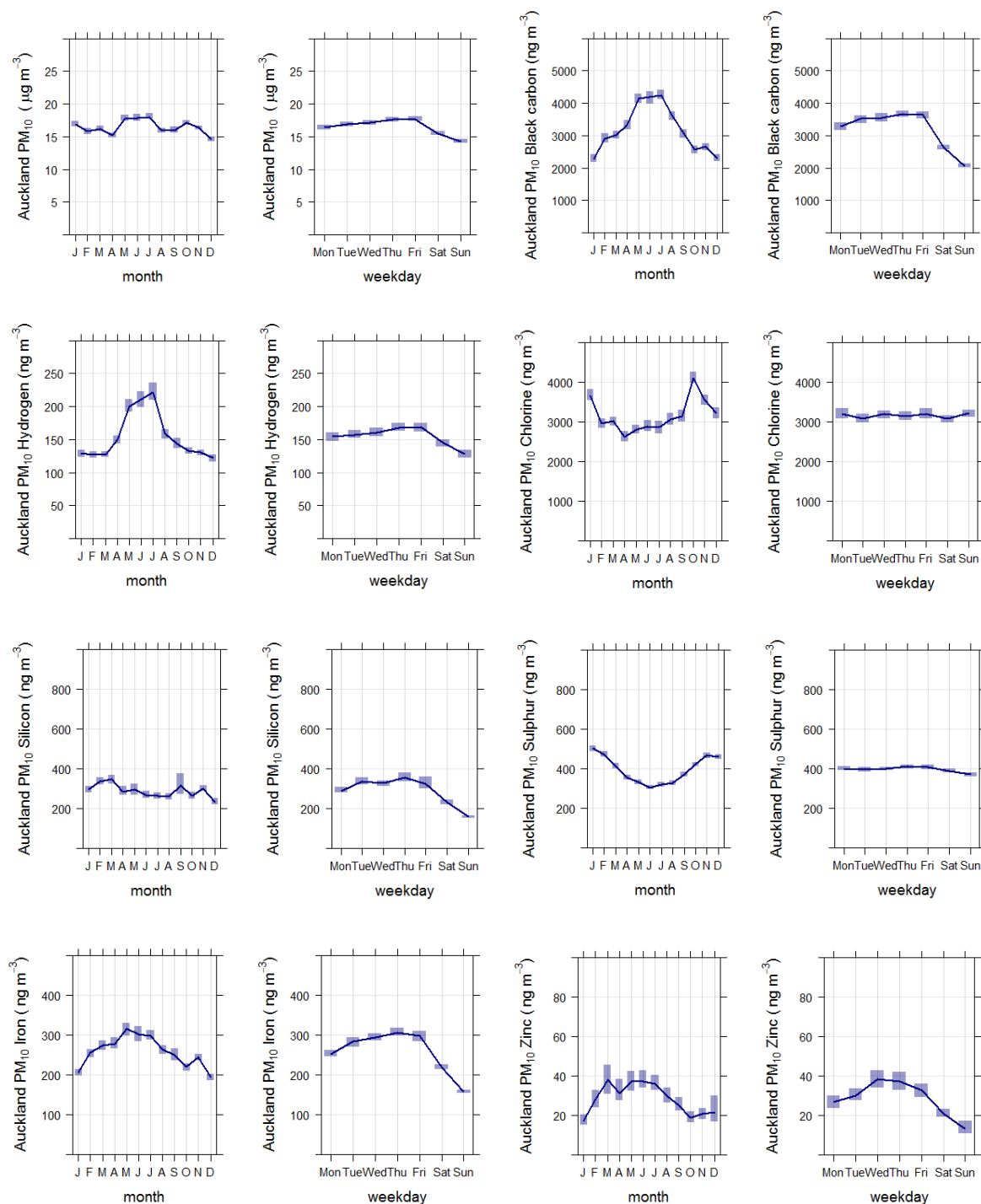


Figure 3.9 Temporal variation analysis for pan-Auckland PM₁₀ concentrations and key PM₁₀ elemental components.

4.0 WESTLAKE GIRLS HIGH SCHOOL, TAKAPUNA

4.1 Site Description

Samples of airborne particles were collected at an ambient air quality monitoring station located within the grounds of Westlake Girls High School, off Taharoto Road, Takapuna (Lat: -36.7803; Long: 174.7489). Figure 4.1 shows a map of the local area.

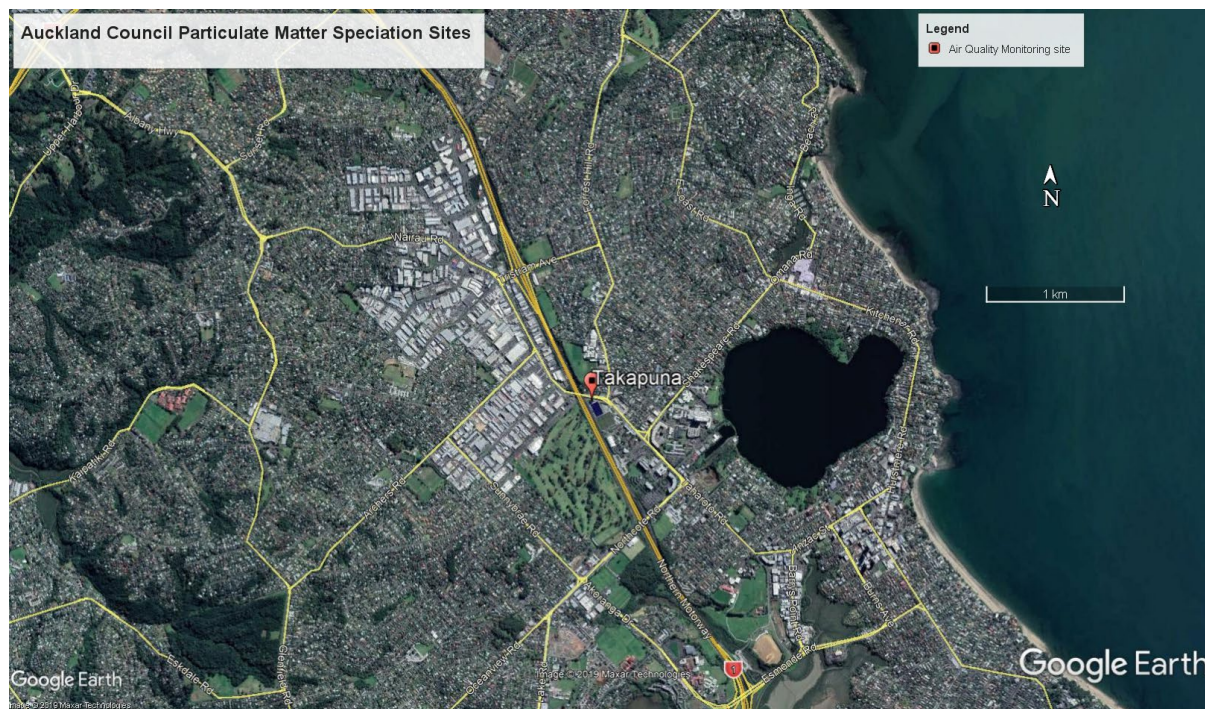


Figure 4.1 Aerial image showing location of Takapuna monitoring site (●) (Source Google Earth).

The Westlake Girls High School site was operated by ML for Auckland Council as part of the council's ambient air quality monitoring programme. The site was established in mid-1995 and is classed as a peak-residential site. Pollutants monitored at the site include CO, NO_x, PM_{2.5} (RAAS speciation sampler) and PM₁₀ (Beta Gauge and Partisol), as well as meteorological parameters.

4.2 Air Particulate Matter Samples and Monitoring Period

Filter samples from two instruments located at the Takapuna air quality monitoring station were supplied by Auckland Council for analysis:

1. 1164 PM_{2.5} samples from an Anderson RAAS speciation sampler on a 1-day-in-3 sampling regime for the period November 2006 to June 2016.
2. 1448 PM₁₀ samples from a Partisol 2000 sampler on a 1-day-in-3 sampling regime for the period December 2005 to January 2021.

4.2.1 Elemental Analysis of PM_{2.5} Samples from the Takapuna Site

Elemental concentrations for PM_{2.5} at the Takapuna site are listed in Table 4.1, with a correlation plot of key elemental concentrations shown in Figure 4.2. (Note that '#>LOD' means the number of samples with concentrations greater than the limit of detection).

Table 4.1 Elemental analysis results for PM_{2.5} at the Takapuna site (1124 samples). PM_{2.5} data is in (µg/m³); elemental data is in ng/m³.

Species	Average	Max.	Min.	Std Dev.	Median	Average LOD	#>LOD
PM_{2.5}	6	35	0	6	4		
H	106	983	0	88	90	46	929
BC	2531	16281	0	2001	2011	178	1157
Na	706	4148	0	543	664	265	871
Mg	71	364	0	59	53	28	978
Al	24	432	0	21	22	14	877
Si	58	1267	17	49	49	10	1164
P	6	34	0	4	7	13	299
S	215	1069	0	179	122	9	1162
Cl	972	5517	6	772	802	6	1163
K	62	1458	0	44	72	7	1154
Ca	44	730	3	39	31	7	1159
Sc	2	23	0	1	3	8	63
Ti	3	31	0	1	3	8	177
V	1	12	0	0	2	8	44
Cr	2	44	0	1	3	7	119
Mn	2	35	0	1	3	7	120
Fe	67	351	0	59	48	5	1144
Co	2	15	0	0	2	9	67
Ni	2	20	0	0	3	9	83
Cu	5	31	0	4	5	10	303
Zn	14	519	0	8	29	12	468
Ga	3	52	0	0	5	18	78
Ge	4	132	0	0	8	23	73
As	5	59	0	0	9	30	101
Se	8	160	0	0	12	36	113
Br	9	182	0	0	15	47	118
Rb	14	111	0	0	21	76	96
Sr	18	212	0	0	27	96	81
Mo	47	553	0	0	83	215	139
I	10	69	0	5	13	27	169
Ba	8	134	0	4	11	29	112
Hg	10	153	0	0	18	67	47
Pb	13	144	0	0	23	82	52

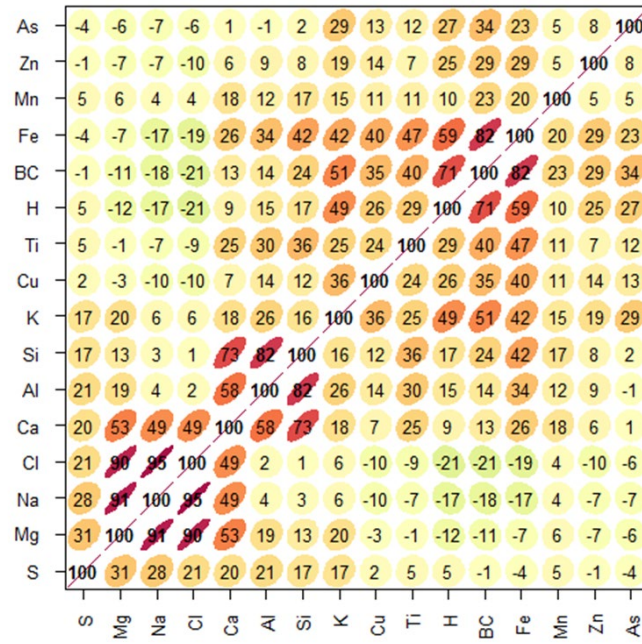


Figure 4.2 Correlation plot for key PM_{2.5} elemental components at the Takapuna site.

4.2.2 Elemental Analysis of PM₁₀ Samples from the Takapuna Site

The Takapuna PM₁₀ samples from the Westlake Girls High School monitoring site refer to those PM₁₀ samples collected from December 2005 to January 2021. Statistics for elemental concentrations in PM₁₀ at the Takapuna site are listed in Table 4.2, with a correlation plot of the key elemental components shown in Figure 4.3.

Table 4.2 Elemental analysis results for PM₁₀ at the Takapuna site (1448 samples). PM₁₀ data is in (µg/m³); elemental data is in ng/m³.

Species	Average	Max.	Min.	Std Dev.	Median	Average LOD	#>LOD
PM₁₀	15	55	3	6	15		
H	137	846	0	108	115	43	1271
BC	2594	11610	95	1707	2228	163	1440
Na	1910	9379	0	1286	1680	419	1375
Mg	183	895	0	112	165	37	1389
Al	100	2114	0	100	78	16	1397
Si	285	5259	19	284	217	11	1448
P	17	174	0	19	12	15	770
S	344	1761	0	176	316	12	1447
Cl	2936	16774	0	1998	2549	7	1447
K	127	1532	0	80	111	7	1446
Ca	177	3381	0	145	157	7	1445
Sc	4	36	0	5	3	9	289
Ti	16	822	0	26	12	8	977
V	1	17	0	2	0	11	55
Cr	3	84	0	10	0	9	154
Mn	5	31	0	5	4	7	476
Fe	256	1230	2	166	225	5	1445
Co	3	46	0	5	1	12	188
Ni	3	32	0	5	1	9	176
Cu	13	97	0	10	11	9	916
Zn	17	298	0	24	11	11	775
Ga	3	35	0	5	0	17	97
Ge	3	31	0	5	0	22	82
As	6	83	0	10	0	29	156
Se	7	50	0	10	0	35	108
Br	11	95	0	15	5	44	199
Rb	13	130	0	20	0	75	113
Sr	19	262	0	29	0	95	142
Mo	40	429	0	72	0	228	396
I	19	267	0	29	8	31	371
Ba	25	331	0	22	22	30	553
Hg	11	126	0	18	0	62	77
Pb	12	159	0	22	0	78	74

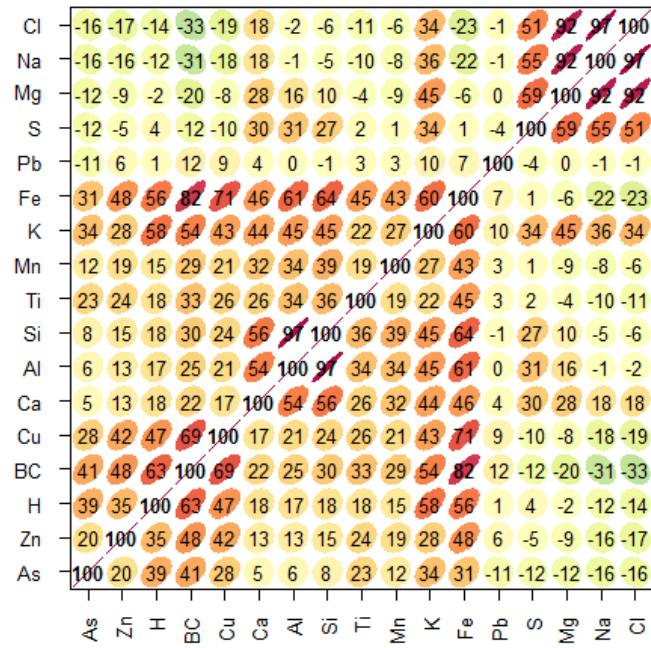


Figure 4.3 Correlation plot for key PM₁₀ elemental components at the Takapuna site.

5.0 QUEEN STREET, CENTRAL AUCKLAND

5.1 Site Description

Samples of airborne particulate matter were collected at an ambient air quality monitoring station located on the veranda over the footpath 4 m above Queen Street (Lat: -36.8476; Long. 174.7655). Figure 5.1 shows an aerial image of the local area.



Figure 5.1 Aerial image showing location of Queen Street monitoring site (●) (Source Google Earth).

5.2 Air Particulate Matter Samples and Monitoring Period

Filter samples from two instruments located at the Queen Street air quality monitoring station were supplied by Auckland Council for analysis:

1. 1127 PM_{2.5} samples from a Partisol sampler on a 1-day-in-3 sampling regime for the period December 2005 to November 2015. Sampling of PM_{2.5} was discontinued at the end of November 2015.
2. 3631 PM₁₀ samples from a Partisol sampler for the period December 2005 to January 2021.

5.2.1 Elemental Analysis of PM_{2.5} Samples from the Queen Street Site

Elemental concentrations for PM_{2.5} at the Queen Street site are listed in Figure 5.1, with a correlation plot of key elemental concentrations shown in Figure 5.2.

Table 5.1 Elemental analysis results for PM_{2.5} at the Queen Street site (1 127 samples). PM_{2.5} data is in (µg/m³); elemental data is in ng/m³.

Species	Average	Max.	Min.	Std Dev.	Median	Average LOD	#>LOD
PM _{2.5}	9	35	1	8	4		
H	124	724	0	116	82	44	947
BC	3133	7923	432	2965	1362	173	1127
Na	684	4068	0	559	593	254	879
Mg	75	567	0	64	55	26	979
Al	36	2895	0	23	99	13	923
Si	75	1831	15	54	85	9	1127
P	7	63	0	4	9	13	277
S	273	1273	37	227	180	9	1127
Cl	917	7042	1	701	826	6	1126
K	64	1990	12	54	75	7	1127
Ca	66	1196	2	52	71	6	1125
Sc	2	23	0	1	3	8	74
Ti	2	51	0	1	4	7	129
V	4	114	0	1	8	7	271
Cr	2	11	0	1	2	6	104
Mn	2	46	0	1	3	6	158
Fe	63	441	3	53	43	5	1123
Co	2	12	0	0	2	9	72
Ni	3	209	0	1	7	8	166
Cu	5	221	0	3	8	10	250
Zn	15	187	0	9	20	11	531
Ga	3	25	0	0	5	17	89
Ge	4	42	0	0	6	22	73
As	4	45	0	0	8	29	84
Se	7	57	0	0	10	34	97
Br	8	71	0	0	12	45	86
Rb	14	109	0	0	20	72	98
Sr	18	123	0	0	26	90	100
Mo	42	393	0	0	71	241	114
I	10	89	0	5	13	25	165
Ba	9	217	0	4	13	27	103
Hg	9	119	0	0	16	63	36
Pb	12	148	0	0	22	77	58

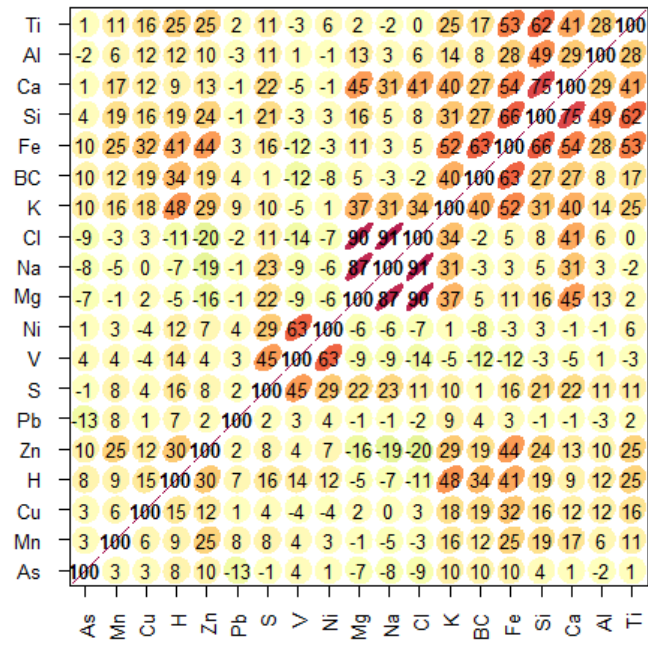


Figure 5.2 Correlation plot for key PM_{2.5} elemental components at the Queen Street site.

5.2.2 Elemental Analysis of PM₁₀ Samples from the Queen Street Site

Statistics for elemental concentrations in PM₁₀ at the Queen Street site are listed in Table 5.2, with a correlation plot of the key elemental components shown in Figure 5.3.

Table 5.2 Elemental analysis results for PM₁₀ at the Queen Street site (3631 samples). PM₁₀ data is in (µg/m³); elemental data is in ng/m³.

Species	Average	Max.	Min.	Std Dev.	Median	Average LOD	#>LOD
PM₁₀	17	130	0	17	6		
H	170	2285	0	158	101	44	3390
BC	3767	12651	0	3338	2043	182	3627
Na	2237	8623	0	2075	1289	480	3537
Mg	211	1002	0	196	113	39	3584
Al	98	6415	0	80	133	16	3577
Si	267	16439	19	212	364	11	3631
P	20	1393	0	16	30	15	2087
S	429	2471	0	390	216	13	3626
Cl	3310	13229	0	2968	2007	6	3627
K	132	1617	0	122	74	7	3628
Ca	262	4949	0	218	233	7	3628
Sc	4	46	0	3	5	10	525
Ti	10	395	0	8	12	8	2085
V	4	118	0	0	8	10	649
Cr	2	26	0	0	2	9	303
Mn	4	99	0	3	4	7	1041
Fe	256	4254	0	248	138	5	3629
Co	3	62	0	1	4	12	323
Ni	3	47	0	2	4	9	528
Cu	11	170	0	10	8	9	2107
Zn	19	750	0	14	23	11	2263
Ga	3	36	0	0	5	18	253
Ge	4	51	0	0	6	23	223
As	4	61	0	0	8	30	257
Se	7	74	0	0	10	36	303
Br	12	106	0	5	16	44	531
Rb	13	144	0	0	20	74	306
Sr	19	166	0	0	27	92	361
Mo	40	455	0	0	71	221	837
I	23	282	0	12	34	32	1002
Ba	21	143	0	18	18	31	1162
Hg	11	157	0	0	18	64	164
Pb	12	152	0	0	22	79	174

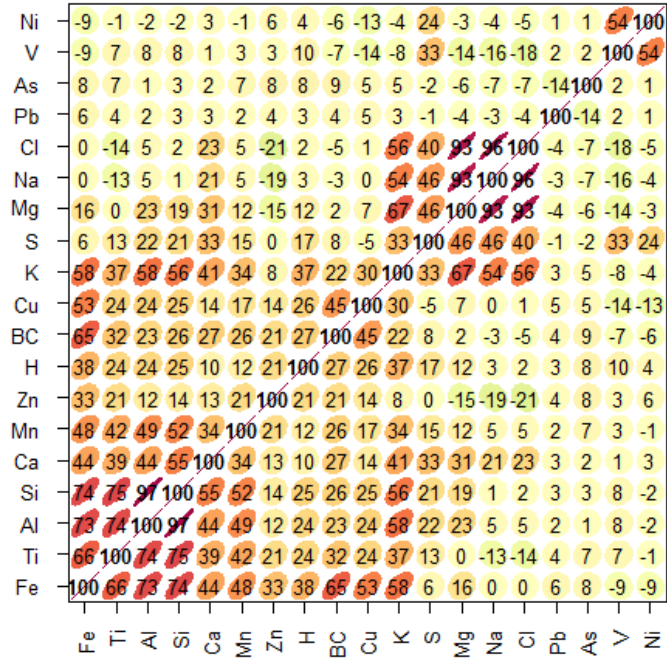


Figure 5.3 Correlation plot for key PM10 elemental components at the Queen Street site.

6.0 KYBER PASS ROAD, NEWMARKET

6.1 Site Description

Samples of airborne particles were collected at an ambient air quality monitoring station on the corner of Khyber Pass Road and Mountain Road, Newmarket (Lat: -36.8662E; Long: 174.7705). Figure 6.1 shows an aerial image of the local area.

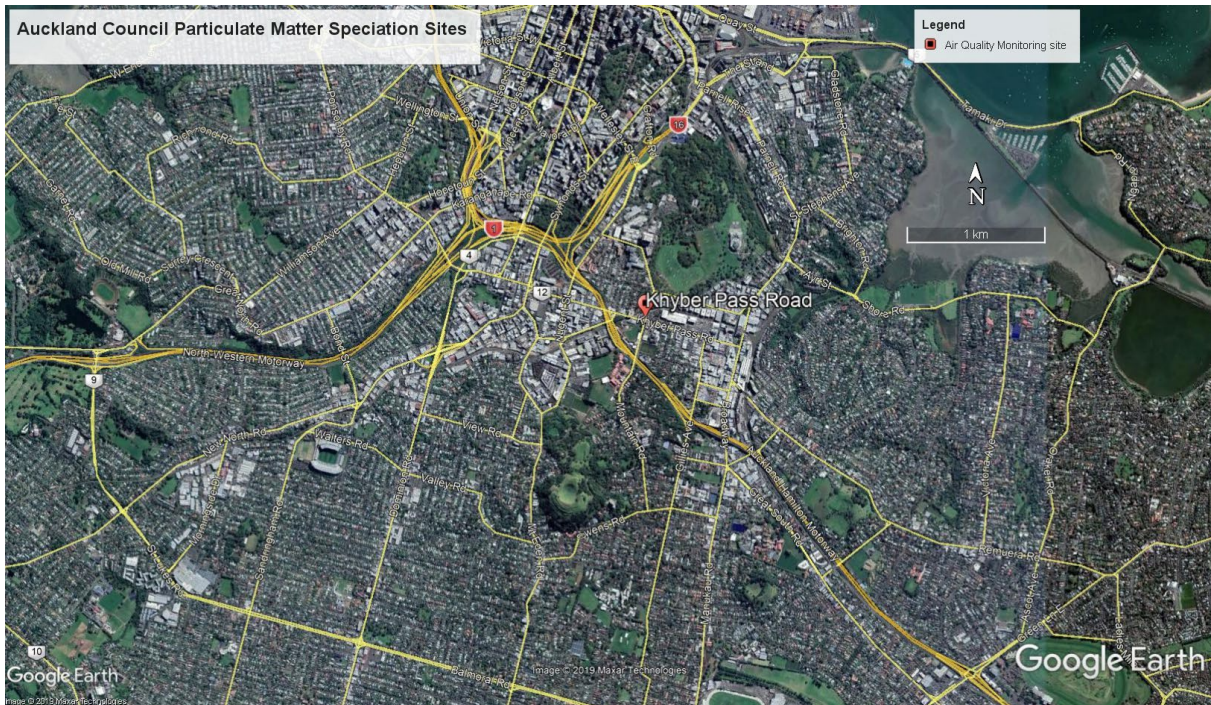


Figure 6.1 Aerial image showing location of Khyber Pass Road monitoring site (●) (Source Google Earth).

6.2 Air Particulate Matter Samples and Monitoring Period

Filter samples from two instruments located at the Khyber Pass Road air quality monitoring station were supplied by Auckland Council for analysis:

1. 1072 PM_{2.5} samples from a Partisol 2000 sampler on a 1-day-in-3 sampling regime for the period December 2005 to April 2015.
2. 1039 PM₁₀ samples from a Partisol 2000 sampler on a 1-day-in-3 sampling regime for the period December 2005 to April 2015.

6.2.1 Elemental Analysis of PM_{2.5} Samples from the Khyber Pass Road Site

Elemental concentrations for PM_{2.5} at the Khyber Pass Road site are listed in Table 6.1, with a correlation plot of key elemental concentrations shown in Figure 6.2.

Table 6.1 Elemental analysis results for PM_{2.5} at the Khyber Pass Road site (1072 samples). PM_{2.5} data is in ($\mu\text{g}/\text{m}^3$); elemental data is in ng/m^3 .

Species	Average	Max.	Min.	Std Dev.	Median	Average LOD	#>LOD
PM _{2.5}	8	40	0	8	4		
H	101	1238	0	88	84	44	850
BC	3719	9152	0	3552	1577	179	1071
Na	516	4605	0	393	512	256	697
Mg	57	643	0	48	50	25	833
Al	25	1603	0	19	55	13	799
Si	66	4435	13	49	173	9	1072
P	6	144	0	4	9	14	248
S	234	2897	33	193	170	8	1072
Cl	678	6040	1	508	646	7	1068
K	57	8100	1	37	265	7	1071
Ca	47	3224	2	38	101	6	1071
Sc	2	26	0	1	2	8	56
Ti	2	125	0	1	5	7	120
V	2	28	0	0	3	7	136
Cr	2	20	0	1	2	6	97
Mn	2	26	0	1	2	6	126
Fe	80	952	4	70	59	5	1071
Co	2	18	0	1	2	9	67
Ni	2	18	0	0	3	8	79
Cu	5	235	0	5	9	9	320
Zn	15	162	0	10	18	11	542
Ga	3	31	0	0	5	17	95
Ge	4	35	0	0	6	21	64
As	4	51	0	0	8	29	78
Se	7	67	0	0	10	34	103
Br	8	399	0	0	17	45	81
Rb	12	114	0	0	20	73	85
Sr	19	238	0	0	28	90	104
Mo	48	488	0	0	78	167	124
I	8	94	0	3	11	25	116
Ba	9	364	0	4	17	27	89
Hg	10	159	0	0	18	62	53
Pb	12	140	0	0	22	77	51

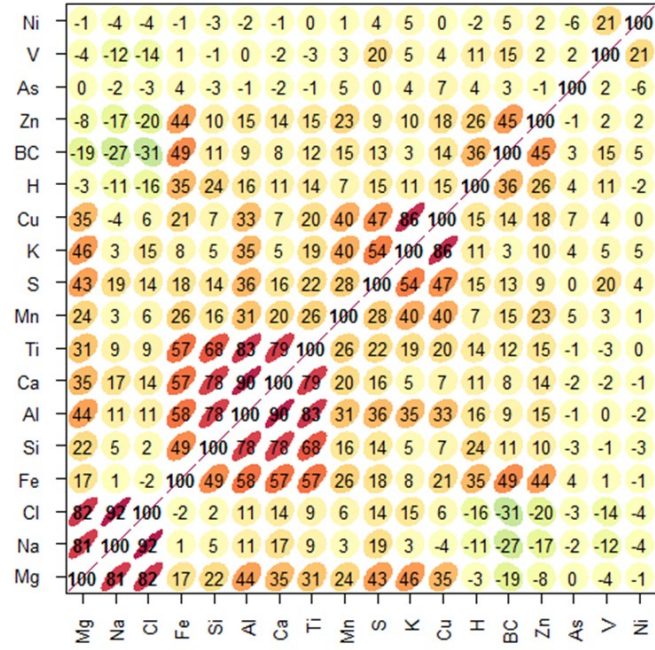


Figure 6.2 Correlation plot for key PM_{2.5} elemental components at the Khyber Pass Road site.

6.2.2 Elemental Analysis of PM₁₀ Samples from the Khyber Pass Road Site

Statistics for elemental concentrations in PM₁₀ at the Khyber Pass Road site are listed in Table 6.2, with a correlation plot of the key elemental components shown in Figure 6.3.

Table 6.2 Elemental analysis results for PM₁₀ at the Khyber Pass Road site (1039 samples). PM₁₀ data is in ($\mu\text{g}/\text{m}^3$); elemental data is in ng/m^3 .

Species	Average	Max.	Min.	Std Dev.	Median	Average LOD	#>LOD
PM ₁₀	18	53	5	17	6		
H	146	823	0	134	97	44	898
BC	4669	14964	0	4402	2206	188	1038
Na	2082	7900	0	1934	1230	449	1000
Mg	204	864	0	188	110	37	1024
Al	125	2003	0	89	150	16	1024
Si	317	5924	35	231	368	11	1039
P	22	136	0	17	21	16	632
S	398	2067	7	370	184	13	1039
Cl	3129	12127	1	2798	1972	7	1038
K	125	4027	4	111	136	7	1038
Ca	210	3922	6	177	175	7	1038
Sc	3	49	0	2	4	10	117
Ti	15	208	0	12	17	7	717
V	2	36	0	0	4	10	86
Cr	2	59	0	0	3	8	138
Mn	6	35	0	5	5	7	439
Fe	421	1713	6	378	226	5	1039
Co	5	54	0	2	7	13	164
Ni	2	56	0	1	3	9	115
Cu	17	90	0	16	11	9	804
Zn	24	297	0	17	27	11	714
Ga	3	30	0	0	5	18	61
Ge	4	37	0	0	6	22	70
As	5	53	0	0	8	29	75
Se	7	64	0	0	10	36	89
Br	11	74	0	5	15	43	130
Rb	14	169	0	0	20	73	81
Sr	18	200	0	0	28	93	94
Mo	44	529	0	0	78	243	102
I	18	225	0	8	28	31	245
Ba	24	245	0	22	19	32	399
Hg	11	114	0	0	18	65	42
Pb	12	111	0	0	21	79	45

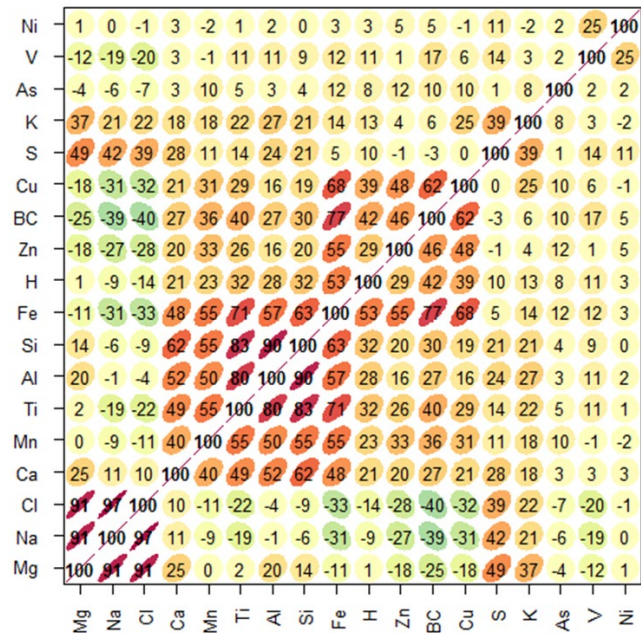


Figure 6.3 Correlation plot for key PM₁₀ elemental components at the Khyber Pass Road site.

7.0 GAVIN STREET, PENROSE

7.1 Site Description

Samples of particulate matter were collected at an ambient air quality monitoring station located at the Gavin Street electricity substation, Penrose (Lat: -36.9045; Long: 174.8156). Figure 7.1 shows an aerial image of the local area.



Figure 7.1 Aerial image showing location of Penrose monitoring site (●) (Source Google Earth).

The Penrose site is operated by WSL for Auckland Council as part of its ambient air quality monitoring programme. The site was established at the end of 2000 and is classed as a peak-residential site. Pollutants monitored include NO_x, PM₁₀ (BAM, HiVol), SO₂, TSP/Lead (HD MedVol), Partisol Speciation Sampling and meteorological parameters.

7.2 Air Particulate Matter Samples and Monitoring Period

Filter samples from two instruments located at the Penrose air quality monitoring station were supplied by Auckland Council for analysis. Sampling for particulate matter composition was terminated in June 2016.

1. 1044 PM_{2.5} samples from a Partisol 2300 speciation sampler collected on a 1-day-in-3 basis for the period January 2006 to June 2016.
2. 1028 PM₁₀ samples from a Partisol 2300 speciation sampler collected on a 1-day-in-3 basis for the period May 2006 to June 2016.
3. 1033 PM₁₀ samples from a Partisol 2000 sampler collected on a 1-day-in-3 basis for the period January 2007 to June 2016.

7.2.1 Elemental Analysis of PM_{2.5} Samples from the Penrose Site

Elemental concentrations for PM_{2.5} at the Penrose site are listed in Table 7.1, with a correlation plot of key elemental concentrations shown in Figure 7.2.

Table 7.1 Elemental analysis results for PM_{2.5} at the Penrose site (1044 samples). PM_{2.5} data is in (µg/m³); elemental data is in ng/m³.

Species	Average	Max.	Min.	Std Dev.	Median	Average LOD	#>LOD
PM _{2.5}	7	40	0	6	5		
H	103	909	0	81	103	41	774
BC	2284	9092	0	2037	1466	172	1037
Na	232	4175	0	101	379	240	389
Mg	29	427	0	23	32	26	505
Al	20	152	0	17	16	13	709
Si	51	460	0	42	33	9	1043
P	4	41	0	1	6	14	160
S	201	1058	0	159	143	8	1040
Cl	330	6968	0	191	493	7	1020
K	43	1112	0	26	66	7	989
Ca	27	272	0	21	23	6	990
Sc	2	14	0	1	2	8	64
Ti	2	48	0	0	3	8	89
V	1	12	0	0	2	7	49
Cr	2	16	0	1	2	6	124
Mn	2	37	0	1	3	6	161
Fe	37	274	0	25	38	5	972
Co	2	13	0	0	2	8	51
Ni	2	13	0	0	2	9	83
Cu	3	87	0	2	5	10	145
Zn	30	521	0	12	51	11	589
Ga	3	41	0	0	5	17	87
Ge	4	33	0	0	6	22	63
As	6	69	0	0	9	29	95
Se	7	60	0	0	10	35	91
Br	9	103	0	0	14	44	119
Rb	15	113	0	0	21	71	111
Sr	18	193	0	0	28	92	102
Mo	42	449	0	0	74	207	105
I	8	71	0	3	10	25	111
Ba	6	120	0	1	10	27	65
Hg	10	120	0	0	18	64	43
Pb	15	214	0	0	26	78	74

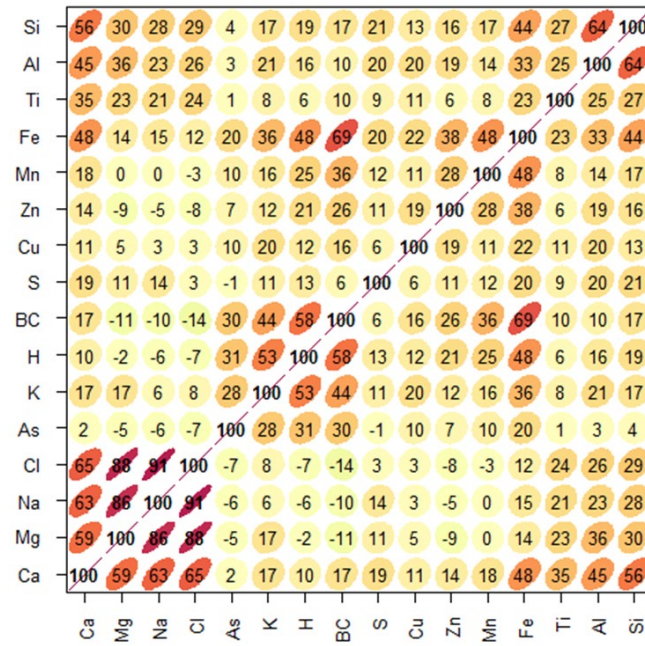


Figure 7.2 Correlation plot for key PM_{2.5} elemental components at the Penrose site.

7.2.2 Elemental Analysis of PM₁₀ Samples from the Penrose Site

Statistics for elemental concentrations in PM₁₀ at the Penrose site are listed in Table 7.2, with a correlation plot of the key elemental components shown in Figure 7.3.

Table 7.2 Elemental analysis results for PM₁₀ at the Penrose site (1028 samples). PM₁₀ data is in (µg/m³); elemental data is in ng/m³.

Species	Average	Max.	Min.	Std Dev.	Median	Average LOD	#>LOD
PM₁₀	17	55	0	16	7		
H	154	1416	0	127	128	41	903
BC	2377	9474	0	2122	1490	176	1021
Na	2015	7529	0	1864	1313	450	938
Mg	202	643	0	188	122	38	961
Al	128	870	0	92	117	16	975
Si	337	2158	18	225	317	11	1028
P	19	146	0	12	21	16	514
S	402	1459	0	368	211	13	1024
Cl	3124	12736	0	2666	2268	7	1023
K	131	1431	0	120	85	7	1016
Ca	224	1197	0	188	157	7	1016
Sc	4	38	0	3	5	10	128
Ti	17	161	0	11	20	8	602
V	1	13	0	0	2	11	33
Cr	3	401	0	0	14	9	176
Mn	6	40	0	4	7	7	370
Fe	237	1415	0	173	210	6	1020
Co	3	41	0	1	5	12	104
Ni	2	107	0	1	5	9	76
Cu	8	117	0	6	8	10	378
Zn	46	698	0	17	72	11	660
Ga	3	46	0	0	5	18	76
Ge	4	37	0	0	6	23	68
As	6	72	0	0	10	29	111
Se	7	60	0	0	10	36	83
Br	12	109	0	4	15	45	124
Rb	14	123	0	0	21	74	80
Sr	20	183	0	0	29	93	104
Mo	41	470	0	0	75	207	96
I	19	343	0	7	31	32	247
Ba	19	130	0	14	20	34	250
Hg	11	161	0	0	19	66	45
Pb	13	257	0	0	25	81	58

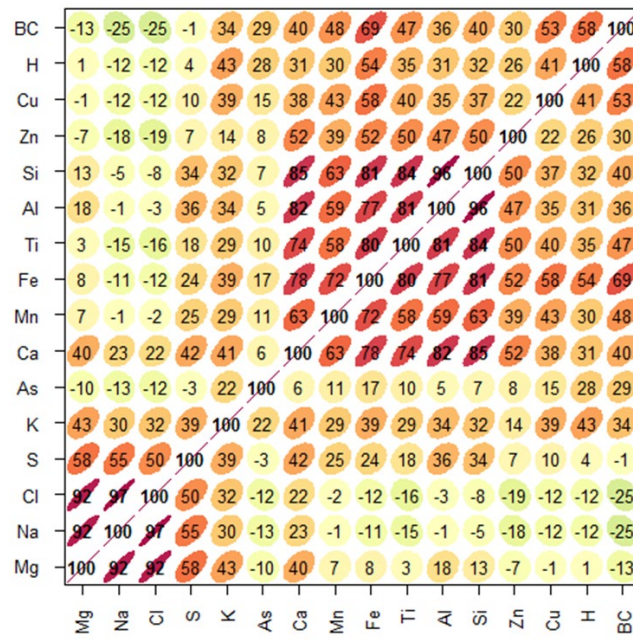


Figure 7.3 Correlation plot for key PM₁₀ elemental components at the Penrose site.

7.2.3 Elemental Analysis of Partisol PM₁₀ Samples from the Penrose Site

Statistics for elemental concentrations in Partisol PM₁₀ at the Penrose site are listed in Table 7.3, with a correlation plot of the key elemental components shown in Figure 7.4.

Table 7.3 Elemental analysis results for PM₁₀ at the Penrose site (1033 samples). PM₁₀ data is in (μg/m³); elemental data is in ng/m³.

Species	Average	Max.	Min.	Std Dev.	Median	Average LOD	#>LOD
PM ₁₀	16	50	0	15	6		
H	141	1016	0	115	117	40	923
BC	2264	8588	0	2084	1471	158	1014
Na	1935	6184	0	1744	1211	489	982
Mg	183	596	0	165	106	37	1003
Al	127	1921	0	92	125	16	987
Si	360	4692	17	251	350	11	1033
P	19	179	0	10	25	15	466
S	357	1205	0	323	175	12	1027
Cl	2945	11838	0	2619	1938	6	1028
K	123	1087	0	113	66	7	1027
Ca	232	2325	0	186	165	7	1030
Sc	5	47	0	3	6	10	200
Ti	19	211	0	14	21	7	712
V	1	12	0	0	2	10	50
Cr	4	98	0	1	7	8	208
Mn	6	36	0	4	6	7	401
Fe	244	1501	0	190	193	6	1028
Co	4	25	0	2	5	11	126
Ni	2	17	0	1	3	10	82
Cu	9	945	0	6	30	11	370
Zn	44	754	0	18	72	13	653
Ga	4	35	0	0	6	20	81
Ge	4	38	0	0	7	26	60
As	5	59	0	0	9	33	83
Se	8	69	0	0	12	39	107
Br	12	100	0	5	16	48	110
Rb	14	106	0	0	21	77	84
Sr	20	180	0	0	29	95	103
Mo	26	325	0	0	60	273	58
I	18	336	0	0	38	33	175
Ba	16	144	0	12	16	30	201
Hg	13	118	0	0	20	71	55
Pb	14	129	0	0	25	89	53

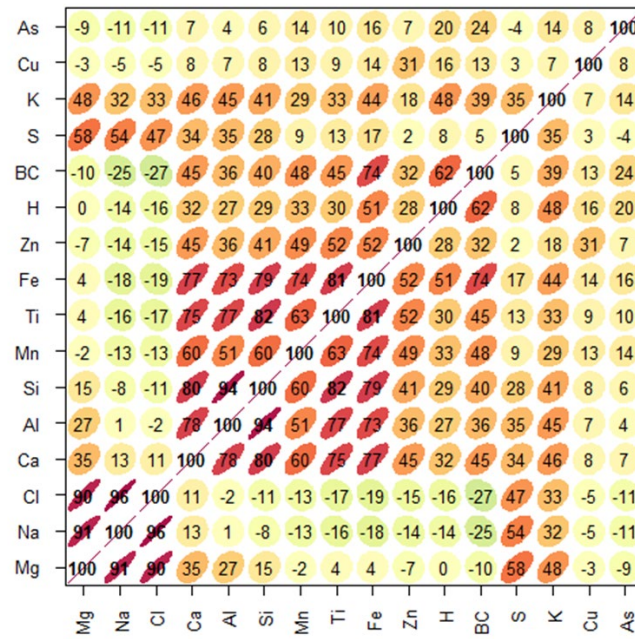


Figure 7.4 Correlation plot for key Partisol PM₁₀ elemental components at the Penrose site.

8.0 LINCOLN ROAD, HENDERSON

8.1 Site Description

Samples of airborne particles were collected at an ambient air quality monitoring station located within the grounds of Henderson Intermediate School, off Lincoln Road, Henderson (Latitude -36.8681; Longitude 174.6284). Figure 8.1 shows an aerial image of the local area.



Figure 8.1 Aerial view showing location of Henderson monitoring site (●) (Source Google Earth).

The Henderson site is operated by ML for Auckland Council as part of its ambient air quality monitoring programme. The site was established at the end of 1993 and is classed as a peak-residential site. Pollutants monitored at the site include CO, NO_x, PM₁₀ (Beta Gauge and Partisol), as well as meteorological parameters.

8.2 Air Particulate Matter Samples and Monitoring Period

Filter samples from one instrument located at the Henderson air quality monitoring station were supplied by Auckland Council for analysis:

1. 1385 PM₁₀ samples from a Partisol 2000 sampler collected on a 1-day-in-3 basis for the period August 2006 to January 2016, then 1-day-in-6 for the period January 2016 to January 2021.

8.2.1 Elemental Analysis of PM₁₀ Samples from the Henderson Site

Statistics for elemental concentrations in PM₁₀ at the Henderson site are listed in Table 8.1, with a correlation plot of the key elemental components shown in Figure 8.2.

Table 8.1 Elemental analysis results for PM₁₀ at the Henderson site (1385 samples). PM₁₀ data is in (µg/m³); elemental data is in ng/m³.

Species	Average	Max.	Min.	Std Dev.	Median	Average LOD	#>LOD
PM₁₀	13	44	0	13	5		
H	161	855	0	131	126	44	1236
BC	1814	10463	0	1308	1627	165	1330
Na	1842	7731	0	1573	1308	412	1321
Mg	177	777	0	152	112	36	1348
Al	83	2384	0	61	109	15	1326
Si	211	5847	17	159	228	11	1385
P	15	108	0	10	16	13	694
S	341	1549	1	317	169	11	1384
Cl	2813	11231	2	2311	2077	6	1384
K	133	2814	0	111	133	7	1384
Ca	135	787	8	128	65	7	1385
Sc	3	27	0	2	4	9	186
Ti	8	228	0	6	11	7	666
V	1	12	0	0	2	9	51
Cr	4	85	0	0	12	8	175
Mn	4	41	0	3	5	7	390
Fe	148	1551	0	115	126	5	1381
Co	2	23	0	1	3	10	118
Ni	3	80	0	1	5	8	198
Cu	5	124	0	4	7	9	435
Zn	37	2301	0	9	138	11	677
Ga	3	26	0	0	4	17	97
Ge	3	37	0	0	6	22	90
As	7	95	0	0	12	27	212
Se	6	76	0	0	10	34	122
Br	10	67	0	3	14	43	174
Rb	12	112	0	0	19	72	100
Sr	16	154	0	0	26	90	112
Mo	38	452	0	0	69	217	352
I	16	213	0	6	25	28	272
Ba	13	313	0	9	18	29	228
Hg	10	107	0	0	17	62	67
Pb	13	166	0	0	24	78	93

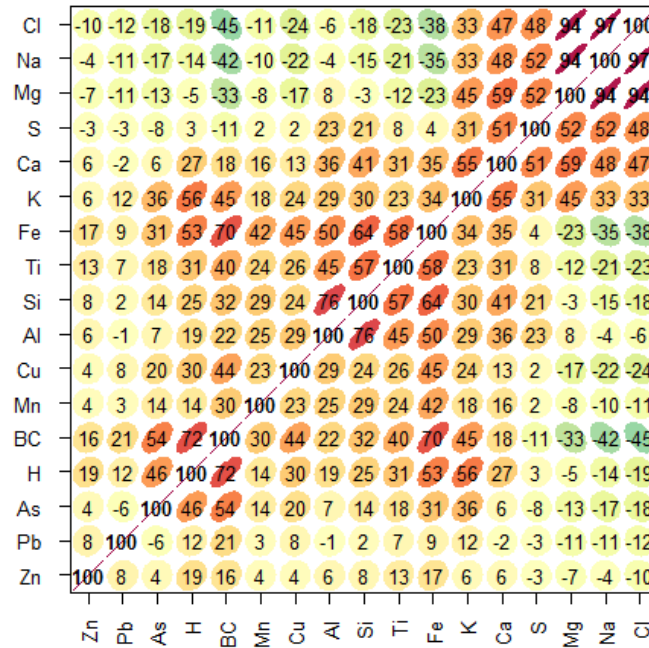


Figure 8.2 Correlation plot for key PM₁₀ elemental components at the Henderson site.

8.3 Re-Analysis of Henderson Filters by X-Ray Fluorescence Spectroscopy

XRF was used to re-measure elemental concentrations in all Henderson PM₁₀ samples collected on Teflon filters. XRF is a complimentary nuclear analytical technique to IBA, providing similar elemental concentration data but with a greater sensitivity to heavier elements, such as arsenic and lead, so that the limits of detection are below the New Zealand Ambient Air Quality Guidelines (NZAAQG; Ministry for the Environment and Ministry of Health 2002), and therefore the concentration data for these two contaminants can be compared directly with the NZAAQG.

XRF measurements in this study were carried out at the GNS Science XRF facility using a PANalytical Epsilon 5 spectrometer (PANalytical, the Netherlands). Further details on the XRF analytical technique are provided in Appendix 1.

Table 8.2 presents the XRF elemental concentration results for the 2007–2021 PM₁₀ samples from Henderson.

Table 8.2 Elemental concentrations by XRF in PM₁₀ samples from the Henderson site (1392 samples). PM₁₀ data is in (µg/m³); elemental data is in ng/m³.

Element	Average	Max.	Min.	Std Dev.	Median	Average LOD	#>LOD
PM ₁₀	13	44	0	13	5		
H	157	855	0	128	128	44	1213
BC	1851	10463	0	1342	1651	165	1329
Na	1272	4531	0	1105	837	6	1384
Mg	146	637	0	132	80	7	1382
Al	165	3651	0	147	138	10	1377
Si	188	6193	0	144	223	4	1381
P	0	15	0	0	1	2	67
S	294	1423	0	272	150	8	1382
Cl	2617	10702	0	2163	1948	0.9	1391
K	125	2388	0	106	118	2	1389
Ca	104	723	0	98	57	3	1384
Ti	10	172	0	8	9	2	1205
V	0	6	0	0	1	0.4	425
Cr	1	265	0	0	8	1	141
Mn	4	125	0	3	6	2	896
Fe	113	3391	0	81	145	6	1164
Co	0	2	0	0	0	0.5	228
Ni	1	131	0	0	4	0.6	443
Cu	5	374	0	4	12	2	995
Zn	36	2283	0	7	134	1	1229
Ga	0	5	0	0	1	1	99
As	6	105	0	0	12	1	524
Se	1	135	0	0	5	1	242
Br	6	35	0	4	5	0.3	1275
Sr	3	60	0	2	3	1	927
Mo	1	15	0	0	2	2	322
Cd	8	62	0	3	10	8	506
Sn	6	82	0	5	7	5	672
Sb	5	35	0	3	6	6	456
Te	7	40	0	5	7	8	501
Cs	9	83	0	4	13	14	394
Ba	13	285	0	7	20	19	379
La	13	129	0	5	18	15	482
Ce	53	607	0	0	84	167	155
Sm	37	382	0	0	63	107	202
Pb	5	45	0	4	6	2	830

From the XRF elemental data for both arsenic and lead, it can be seen very clearly that the heavy metals show winter concentration maxima at the Henderson monitoring site, as presented in Figure 8.3.

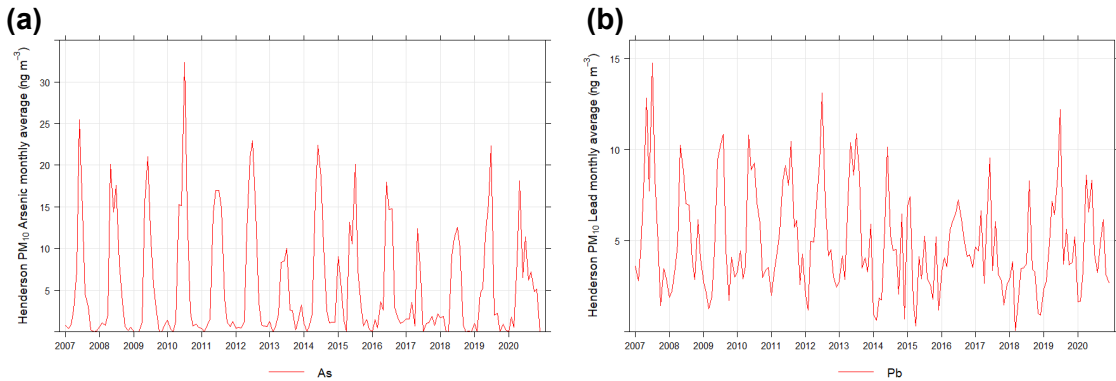


Figure 8.3 Monthly average arsenic (a) and lead (b) concentrations in PM₁₀ at the Henderson air quality monitoring site.

The last three years of data indicate that annual average concentrations for arsenic at Henderson (Figure 8.4) have exceeded the AAQG (5.5 ng m⁻³), but the long-term record shows inter-annual variability around, with some years exceeding the AAQG and some years below. The inter-annual variation was likely to be a combination of meteorological influences and source activity (i.e. the amount of CCA-treated timber being burnt in local fireplaces). At other New Zealand urban centres with colder winters and a greater prevalence of domestic solid fuel fires used for home heating, the concentrations of arsenic were found to be commensurately higher than those shown for Henderson (Davy and Trompetter 2018).



Figure 8.4 Annual average arsenic concentrations at Henderson.

Another more intermittent source of heavy metals at Henderson appears to be associated with fireworks events (Rindelaub et al. 2021); coincident peaks in Sr, K, Cu, Ba, V and Ti, all of which are components of pyrotechnics, suggest that lead is used in at least some firework products, most likely as lead nitrate due to its properties as an oxidiser when heated (Conkling 2000).

The long-term trends in arsenic and lead concentrations at Henderson are presented in Figures 8.5 and 8.6, respectively.

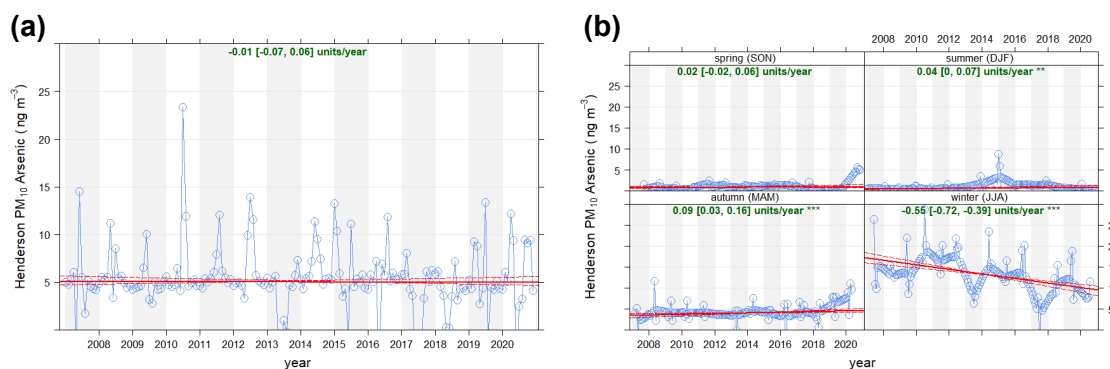


Figure 8.5 Trend analysis for arsenic concentrations at Henderson; (a) de-seasonalised and (b) seasonal trends.

The trend analysis for arsenic shows higher winter concentrations (Figure 8.5b) and that there has been a statistically significant (99.9 percentile confidence intervals) decrease during the winter seasons but increasing concentrations during autumn. The long-term de-seasonalised average (Figure 8.5a) shows no statistically significant trend.

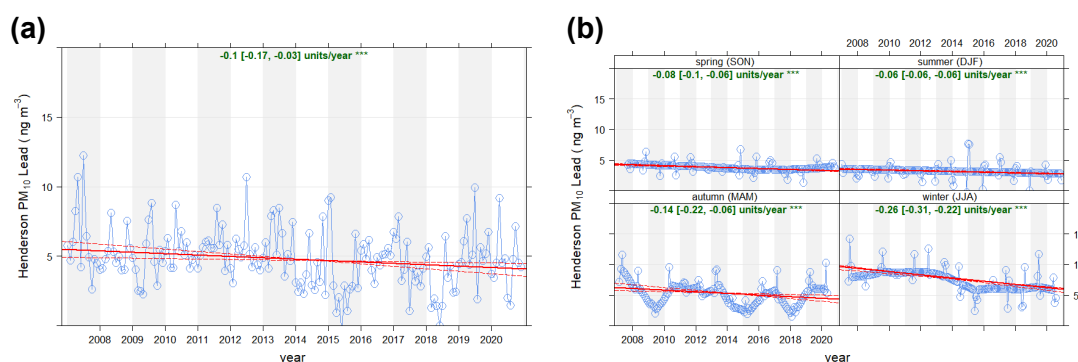


Figure 8.6 Trend analysis for lead concentrations at Henderson; (a) de-seasonalised and (b) seasonal trends.

Lead concentrations at Henderson show a statistically significant (99.9 percentile confidence intervals) decrease between 2007 and 2021 (Figure 8.6a) across all seasons, with the greatest decrease during winter, as shown in Figure 8.6b, suggesting that the use of old painted timber as fuel for domestic fires is decreasing.

9.0 REFERENCES

- Cahill TA, Eldred RA, Motallebi N, Malm WC. 1989. Indirect measurement of hydrocarbon aerosols across the United States by nonsulfate hydrogen-remaining gravimetric mass correlations. *Aerosol Science and Technology*. 10(2):421–429. doi:10.1080/02786828908959281.
- Cahill TA, Eldred RA, Wilkinson LK, Perley BP, Malm WC. 1990. Spatial and temporal trends of fine particles at remote U.S. sites. In: *Proceedings: 83rd Air & Waste Management Association Annual Meeting*; 1990 Jun 24–29; Pittsburgh, Pennsylvania. [Place unknown]: Air & Waste Management Association.
- Cohen DD. 1998. Characterisation of atmospheric fine particles using IBA techniques. *Nuclear Instruments and Methods in Physics Research Section B: Beam Interactions with Materials and Atoms*. 136–138:14–22. doi:10.1016/S0168-583X(97)00658-7.
- Cohen D. 1999. Accelerator based ion beam techniques for trace element aerosol analysis. In: Landsberger S, Creatchman M, editors. *Elemental analysis of airborne particles*. Amsterdam (NL): Gordon and Breach Science Publishers. p. 139–196. (Advances in environmental, industrial, and process control technologies; 1).
- Cohen DD, Bailey GM, Kondepudi R. 1996. Elemental analysis by PIXE and other IBA techniques and their application to source fingerprinting of atmospheric fine particle pollution. *Nuclear Instruments and Methods in Physics Research Section B: Beam Interactions with Materials and Atoms*. 109–110:218–226. doi:10.1016/0168-583X(95)00912-4.
- Cohen DD, Garton D, Stelcer E. 2000. Multi-elemental methods for fine particle source apportionment at the global baseline station at Cape Grim, Tasmania. *Nuclear Instruments and Methods in Physics Research Section B: Beam Interactions with Materials and Atoms*. 161–163:775–779. doi:10.1016/S0168-583X(99)00910-6.
- Conkling JA. 2000. *Pyrotechnics*. Kirk-Othmer Encyclopedia of Chemical Technology.
- Davy PK, Trompetter WJ. 2018. Heavy metals, black carbon and natural sources of particulate matter in New Zealand. Lower Hutt (NZ): GNS Science. 81 p. Consultancy Report 2017/238. Prepared for Ministry for the Environment.
- Davy PK, Trompetter WJ. 2020. Composition, sources and long-term trends for Auckland air particulate matter: summary report. Lower Hutt (NZ): GNS Science. 32 p. + appendices. Consultancy Report 2019/151. Prepared for Auckland Council.
- Fine PM, Cass GR, Simoneit BRT. 2001. Chemical characterization of fine particle emissions from fireplace combustion of woods grown in the northeastern United States. *Environmental Science & Technology*. 35(13):2665–2675. doi:10.1021/es001466k.
- Horvath H. 1993. Atmospheric light absorption: a review. *Atmospheric Environment Part A General Topics*. 27(3):293–317. doi:10.1016/0960-1686(93)90104-7.
- Horvath H. 1997. Experimental calibration for aerosol light absorption measurements using the integrating plate method – summary of the data. *Journal of Aerosol Science*. 28(7):1149–1161. doi:10.1016/S0021-8502(97)00007-4.
- Jacobson MC, Hansson HC, Noone KJ, Charlson RJ. 2000. Organic atmospheric aerosols: review and state of the science. *Reviews of Geophysics*. 38(2):267–294. doi:10.1029/1998RG000045.
- Kara M, Hopke P, Dumanoglu Y, Altioik H, Elbir T, Odabasi M, Bayram A. 2015. Characterization of PM using multiple site data in a heavily industrialized region of Turkey. *Aerosol and Air Quality Research*. 15(1):11–27. doi:10.4209/aaqr.2014.02.0039.

- Lee E, Chan CK, Paatero P. 1999. Application of positive matrix factorization in source apportionment of particulate pollutants in Hong Kong. *Atmospheric Environment*. 33(19):3201–3212. doi:10.1016/S1352-2310(99)00113-2.
- Maenhaut W, Malmqvist KG. 2001. Particle-induced X-ray emission analysis. In: van Grieken R, Markowicz A, editors. *Handbook of X-ray spectrometry*. 2nd ed. New York (NY): Marcel Dekker. p. 719–810.
- Malm WC, Sisler JF, Huffman D, Eldred RA, Cahill TA. 1994. Spatial and seasonal trends in particle concentration and optical extinction in the United States. *Journal of Geophysical Research: Atmospheres*. 99(D1):1347–1370. doi:10.1029/93jd02916.
- Maxwell JA, Campbell JL, Teesdale WJ. 1989. The Guelph PIXE software package. *Nuclear Instruments and Methods in Physics Research Section B: Beam Interactions with Materials and Atoms*. 43(2):218–230. doi:10.1016/0168-583X(89)90042-6.
- Maxwell JA, Teesdale WJ, Campbell JL. 1995. The Guelph PIXE software package II. *Nuclear Instruments and Methods in Physics Research Section B: Beam Interactions with Materials and Atoms*. 95(3):407–421. doi:10.1016/0168-583X(94)00540-0.
- Ministry for the Environment, Ministry of Health. 2002. Ambient air quality guidelines: 2002 update. Wellington (NZ): Ministry for the Environment. 58 p. (Air Quality Report; 32).
- Patel H, Talbot N, Salmond J, Dirks K, Xie S, Davy P. 2020. Implications for air quality management of changes in air quality during lockdown in Auckland (New Zealand) in response to the 2020 SARS-CoV-2 epidemic. *Science of The Total Environment*. 746:141129. doi:10.1016/j.scitotenv.2020.141129.
- Rindelaub JD, Davy PK, Talbot N, Pattinson W, Miskelly GM. 2021. The contribution of commercial fireworks to both local and personal air quality in Auckland, New Zealand. *Environmental Science and Pollution Research*. 28(17):21650–21660. doi:10.1007/s11356-020-11889-4.
- Salma I, Chi X, Maenhaut W. 2004. Elemental and organic carbon in urban canyon and background environments in Budapest, Hungary. *Atmospheric Environment*. 38(1):27–36. doi:10.1016/j.atmosenv.2003.09.047.
- Trompetter WJ. 2004. Ion beam analysis results of air particulate filters from the Wellington Regional Council. Lower Hutt (NZ): Institute of Geological & Nuclear Sciences. 17 p. Client Report 2004/24. Prepared for Wellington Regional Council.
- Trompetter WJ, Markwitz A, Davy PK. 2005. Air particulate research capability at the New Zealand Ion Beam Analysis Facility using PIXE and IBA techniques. *International Journal of PIXE*. 15(03n04):249–255. doi:10.1142/s0129083505000581.
- Watson JG, Chow JC, Frazier CA. 1999. X-ray fluorescence analysis of ambient air samples. In: Landsberger S, Creatchman M, editors. *Elemental analysis of airborne particles*. Amsterdam (NL): Gordon and Breach Science Publishers. p. 67–96. (Advances in environmental, industrial, and process control technologies; 1).
- Watson JG, Zhu T, Chow JC, Engelbrecht J, Fujita EM, Wilson WE. 2002. Receptor modeling application framework for particle source apportionment. *Chemosphere*. 49(9):1093–1136. doi:10.1016/S0045-6535(02)00243-6.

This page left intentionally blank.

APPENDICES

This page left intentionally blank.

APPENDIX 1 SAMPLE ANALYSIS AND DATA QUALITY ASSURANCE

A1.1 Black Carbon Analysis

Black carbon (BC) has been studied extensively, but it is still not clear to what degree it is elemental carbon [EC (or graphitic) C(0)] or high molecular weight refractory weight organic species or a combination of both (Jacobson et al. 2000). Current literature suggests that BC is likely a combination of both and that, for combustion sources such as petrol- and diesel-fuelled vehicles and biomass burning (wood burning, coal burning), EC and organic carbon compounds (OC) are the principle aerosol components emitted (Fine et al. 2001; Jacobson et al. 2000; Salma et al. 2004; Watson et al. 2002).

Determination of carbon (soot) on filters was performed by light reflection to provide the BC concentration. The absorption and reflection of visible light on particles in the atmosphere or collected on filters is dependent on the particle concentration, density, refractive index and size. For atmospheric particles, BC is the most highly absorbing component in the visible light spectrum, with very much smaller components coming from soils, sulphates and nitrate (Horvath 1993, 1997). Hence, to the first order, it can be assumed that all of the absorption on atmospheric filters is due to BC. The main sources of atmospheric BC are anthropogenic combustion sources and include biomass burning, motor vehicles and industrial emissions (Cohen et al. 2000). Cohen and co-workers found that BC is typically 10–40% of the fine mass (PM_{2.5}) fraction in many urban areas of Australia.

When measuring BC by light reflection/transmission, light from a light source is transmitted through a filter onto a photocell. The amount of light absorption is proportional to the amount of BC present and provides a value that is a measure of the BC on the filter. Conversion of the absorbance value to an atmospheric concentration value of BC requires the use of an empirically derived equation (Cohen et al. 2000):

$$BC (\mu\text{g cm}^{-2}) = (100/2(F\varepsilon)) \ln[R_0/R] \quad \text{Equation A1.1}$$

where:

- ε is the mass absorbent coefficient for BC ($\text{m}^2 \text{g}^{-1}$) at a given wavelength.
- F is a correction factor to account for other absorbing factors, such as sulphates, nitrates, shadowing and filter loading. These effects are generally assumed to be negligible and F is set at 1.00.
- R_0 , R are the pre- and post-reflection intensity measurements, respectively.

BC was measured at GNS Science using the M43D Digital Smoke Stain Reflectometer. The following equation (from Willy Maenhaut, Institute for Nuclear Sciences, University of Gent, Proeftuinstraat 86, B-9000 GENT, Belgium) was used for obtaining BC from reflectance measurements on Nucleopore polycarbonate filters or Pall Life Sciences Teflon filters:

$$BC (\mu\text{g cm}^{-2}) = [1000 \times \text{LOG}(R_{\text{blank}}/R_{\text{sample}}) + 2.39] / 45.8 \quad \text{Equation A1.2}$$

where:

- R_{blank} is the average reflectance for a series of blank filters; R_{blank} is close, but not identical, to 100 (GNS Science always uses the same blank filter for adjusting to 100); and
- R_{sample} is the reflectance for a filter sample (normally lower than 100)

with 2.39 and 45.8 constants derived using a series of 100 Nuclepore polycarbonate filter samples, which served as secondary standards; the BC loading (in $\mu\text{g cm}^{-2}$) for these samples had been determined by Prof. Dr. MO Andreae (Max Planck Institute of Chemistry, Mainz, Germany) relative to standards that were prepared by collecting burning acetylene soot on filters and determining the mass concentration gravimetrically (Trompeter 2004).

A1.2 Elemental Concentrations by Ion Beam Analysis

Ion beam analysis (IBA) was used to measure the elemental concentrations of particulate matter on the size-resolved filter samples from the Coles Place monitoring site. IBA is based on the measurement of characteristic X-rays and γ -rays of an element produced by ion-atom interactions using high-energy protons in the 2–5 million electron volt (MeV) range. IBA is a mature and well-developed science, with many research groups around the world using IBA in a variety of routine analytical applications, including the analysis of atmospheric aerosols (Maenhaut and Malmqvist 2001; Trompeter et al. 2005). IBA techniques do not require sample preparation and are fast, non-destructive and sensitive (Cohen 1999; Maenhaut and Malmqvist 2001; Trompeter et al. 2005).

IBA measurements for this study were carried out at the New Zealand IBA facility operated by GNS Science. Figure A1.1 shows the PM analysis chamber with its associated X-ray, γ -ray and particle detectors for Particle-Induced X-ray Emission (PIXE), Particle-Induced Gamma-ray Emission (PIGE), Proton Elastic Scattering Analysis (PESA) and Rutherford Back Scattering (RBS) measurements.

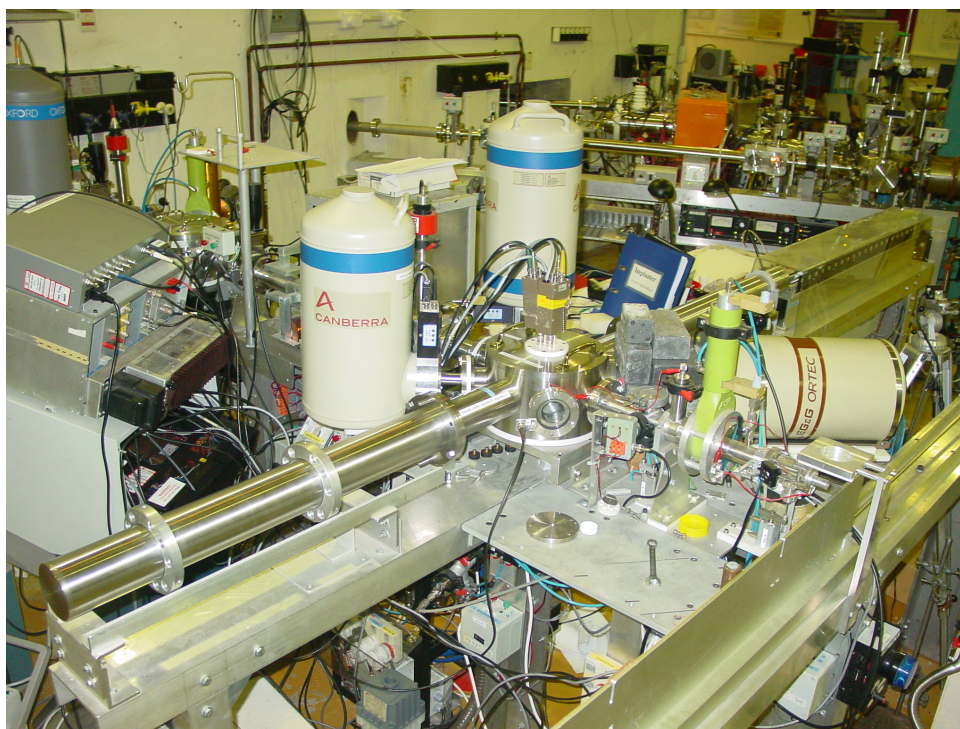


Figure A1.1 Particulate matter analysis chamber with its associated detectors.

The following sections provide a generalised overview of the IBA techniques used for elemental analysis and the analytical set-up at GNS Science (Cohen 1998; Cohen et al. 1996; Trompeter 2004; Trompeter et al. 2005). Figure A1.2 presents a schematic diagram of the typical experimental set-up for IBA of air particulate filters at GNS Science.

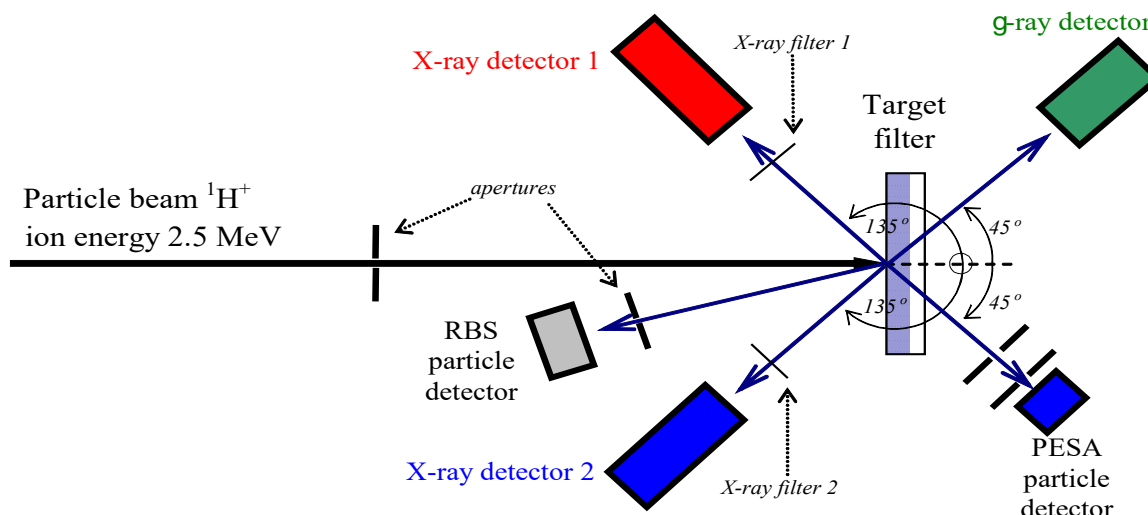


Figure A1.2 Schematic of the typical ion beam analysis experimental set-up at GNS Science.

A1.2.1 Particle-Induced X-Ray Emission

PIXE is used to determine elemental concentrations heavier than neon by exposing the filter samples to a proton beam accelerated to 2.5 million volts (MeV) by the GNS Science 3 MeV van-de-Graaff accelerator. When high-energy protons interact with atoms in the sample, characteristic X-rays (from each element) are emitted by ion-electron processes. These X-rays are recorded in an energy spectrum. While all elements heavier than boron emit K X-rays, their production become too few to satisfactorily measure elements heavier than strontium. Elements heavier than strontium are detected via their lower-energy L X-rays. The X-rays are detected using a Si(Li) detector, and the pulses from the detector are amplified and recorded in a pulse height analyser. In practice, sensitivities are further improved for the lighter elements by using two X-ray detectors, one for light element X-rays and the other for heavier element X-rays, each with different filtering and collimation. Figure A1.3 shows an example of a PIXE spectrum for airborne particles collected on a filter and analysed at the GNS Science IBA facility.

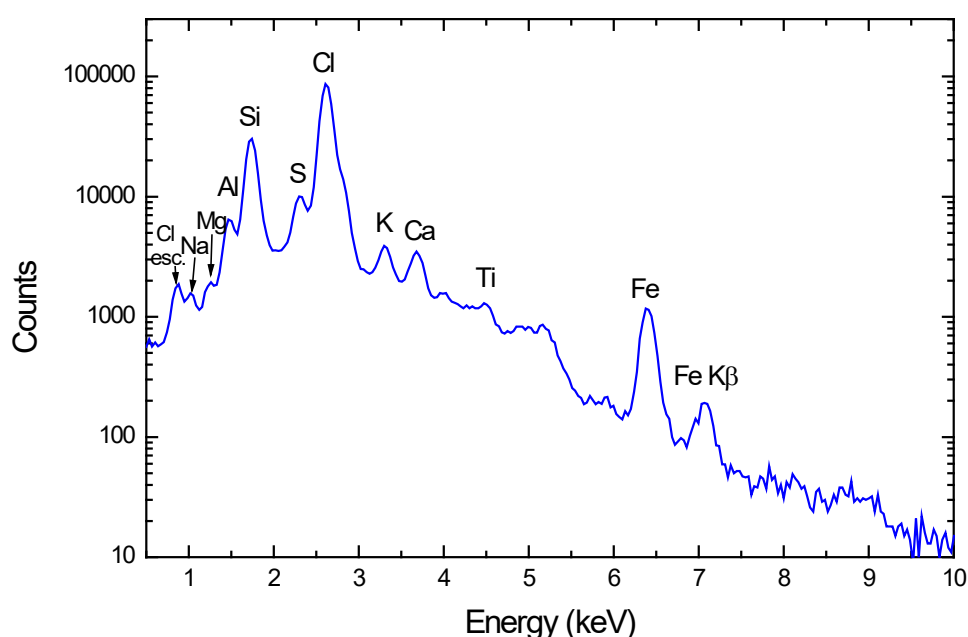


Figure A1.3 Typical particle-induced X-ray emission spectrum for an aerosol sample.

As the PIXE spectrum consists of many peaks from different elements (and a Bremsstrahlung background), some of them overlapping, the spectrum is analysed with quantitative X-ray analysis software. In the case of this study, GUPIX software was used to perform the deconvolution with high accuracy (Maxwell et al. 1989, 1995). The number of pulses (counts) in each peak for a given element is used by the GUPIX software to calculate the concentration of that element. The background and neighbouring elements determine the statistical error and limit of detection (LOD). Note that GUPIX provides a specific statistical error and LOD for each element in any filter, which is essential for source-apportionment studies.

Typically, 20–25 elements from Mg–Pb are routinely determined above their respective LODs. Sodium (and fluorine) was determined using both PIXE and PIGE (see next section). Specific experimental details, where appropriate, are given in the results and analysis section.

A1.2.2 Particle-Induced Gamma-Ray Emission

PIGE refers to γ -rays produced when an incident beam of protons interacts with the nuclei of an element in the sample (filter). During the de-excitation process, nuclei emit γ -ray photons of characteristic energies specific to each element. Typical elements measured with γ -ray are:

Element	Nuclear Reaction	Gamma Ray Energy (keV)
Sodium	$^{23}\text{Na}(p,\alpha\gamma)^{20}\text{Ne}$	440, 1634
Fluorine	$^{19}\text{F}(p,\alpha\gamma)^{16}\text{O}$	197, 6129

Gamma rays are higher in energy than X-rays and are detected with a germanium detector. Measurements of a light element such as sodium can be measured more accurately using PIGE, as the γ -rays are not attenuated to the same extent in the filter matrix or the detector material, a problem in the measurement of low-energy X-rays of sodium. Figure A1.4 shows a typical PIGE spectrum.

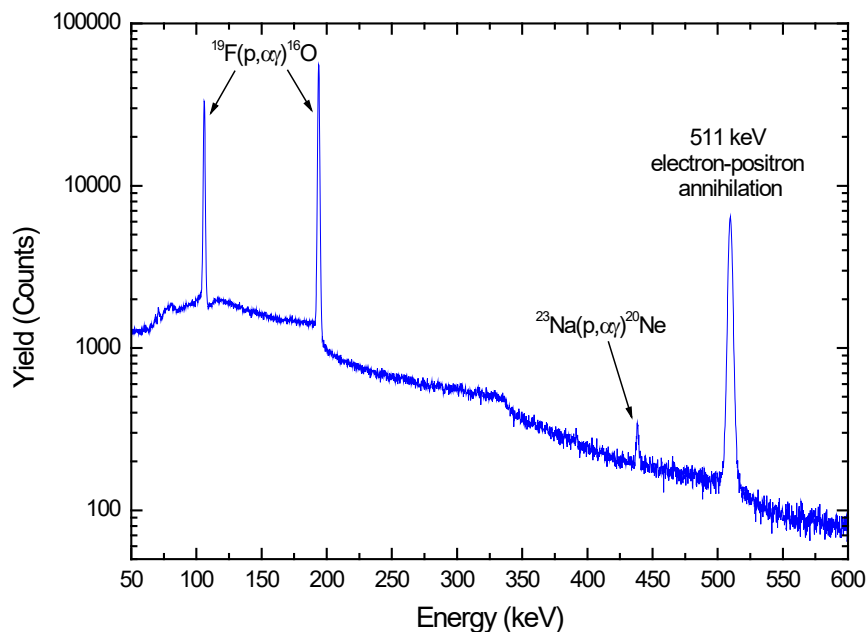


Figure A1.4 Typical particle-induced gamma-ray emission spectrum for an aerosol sample.

A1.3 Elemental Concentrations by X-Ray Fluorescence Spectroscopy

X-ray fluorescence spectroscopy (XRF) was used to measure elemental concentrations in PM₁₀ samples collected on Teflon filters at Henderson. XRF measurements in this study were carried out at the GNS Science XRF facility and the spectrometer used was a PANalytical Epsilon 5 (PANalytical, the Netherlands). The Epsilon 5 is shown in Figure A1.5. XRF is a non-destructive and relatively rapid method for the elemental analysis of particulate matter samples.



Figure A1.5 The PANalytical Epsilon 5 spectrometer.

XRF is based on the measurement of characteristic X-rays produced by the ejection of an inner shell electron from an atom in the sample, creating a vacancy in the inner atomic shell. A higher-energy electron then drops into the lower-energy orbital and releases a fluorescent X-ray to remove excess energy (Watson et al. 1999). The energy of the released X-ray is characteristic of the emitting element, and the area of the fluorescent X-ray peak (intensity of the peak) is proportional to the number of emitting atoms in the sample. From the intensity, it is possible to calculate a specific element's concentration by direct comparison with standards.

To eject inner shell electrons from atoms in a sample, the XRF spectrometer at GNS Science uses a 100 kV Sc/W X-ray tube. The 100 kV X-rays produced by this tube are able to provide elemental information for elements from Na–U. Unlike IBA techniques, which are similar to XRF, the PANalytical Epsilon 5 is able to use characteristic K-lines produced by each element for quantification. This is crucial for optimising LOD, because K-lines have higher intensities and are located in less-crowded regions of the X-ray spectrum. The X-rays emitted by the sample are detected using a high-performance Ge detector, which further improves the detection limits. Figure A1.6 presents a sample X-ray spectrum.

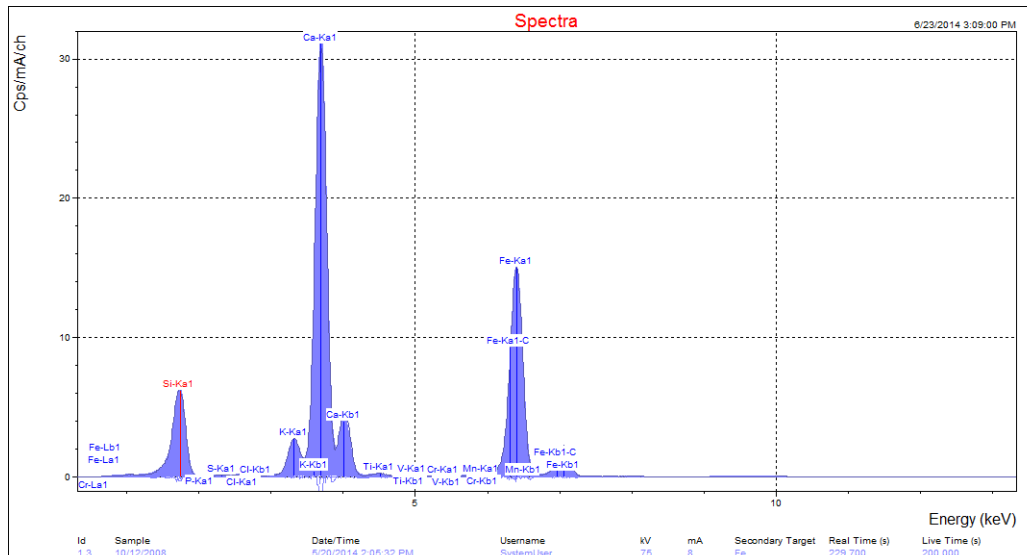


Figure A1.6 Example X-ray spectrum from a PM₁₀ sample.

At GNS Science, calibration standards for each of the elements of interest were analysed prior to the samples being run. Once the calibration standards were analysed, spectral deconvolutions were performed using PANalytical software to correct for line overlaps and ensure that the spectra were accurately fit. Calibration curves for each element of interest were produced and used to determine the elemental concentrations from particulate matter samples. A National Institute of Standards and Technology reference sample (SRM 2783) and multi-elemental reference standards from Crocker National Laboratory (University of California, Davis) were also analysed to ensure that the results obtained were robust and accurate.

A1.4 X-Ray Fluorescence Spectroscopy and Ion Beam Analysis Data Reporting

Most filters used to collect particulate matter samples for XRF or IBA analysis are sufficiently thin enough that the X-rays or ion beam penetrate the entire depth, producing a quantitative analysis of elements present. Because of the thin nature of the air particulate matter filters, the concentrations reported from the analyses are therefore in aerial density units (ng cm^{-2}), and the total concentration of each element on the filters is calculated by multiplying with the exposed area of the filter. Typically, the exposed area is approximately 12 cm^2 for the sample deposit on the standard 47 mm Teflon filters used at Auckland sites. For example, to convert from $\text{Cl} (\text{ng cm}^{-2})$ into $\text{Cl} (\text{ng m}^{-3})$ for filter samples, the equation is:

$$Cl (\text{ng m}^{-3}) = 11.95 (\text{cm}^2) \times Cl (\text{ng cm}^{-2}) / Vol(\text{m}^3).1 \quad \text{Equation A1.3}$$

A1.4.1 Limits of Detection and Uncertainty Reporting for Elements

The exact LOD and associated analytical uncertainties for the concentration of each element depends on a number of factors such as:

- the method of detection
- filter composition
- sample composition
- the detector resolution, and
- spectral interference from other elements.

There are differences in how the analytical LOD and uncertainties are calculated between the XRF and IBA analytical methodologies due to the nature of the measurements and the manner in which the sample spectra are deconvoluted by the associated software. Also, where an individual elemental concentration is reported as zero (0), this means that the measurement value (as derived from the spectral deconvolution) was zero but does not necessarily mean it was not present; rather, it was below the method LOD and indeterminate. Where this is the case, then the corresponding uncertainty value (\pm) can be regarded as 5/6 LOD (Kara et al. 2015):

The following sections give an overview of this process for XRF and IBA, respectively.

A1.4.1.1 Limits of Detection and Uncertainty Reporting for Elements Determined by X-Ray Fluorescence Spectroscopy

For XRF elemental data, the detection limits are defined in terms of the uncertainty in the blank (1σ) of 10 repeat measurements (USEPA Compendium Method IO-3.3). This ignores the effect of other elements, which is generally small due to the use of multiple excitation frequencies, except for the light elements (potassium and lower), where overlapping spectral lines will increase the detection limit.

Uncertainties for the XRF elemental data were calculated using the following equations (Kara et al. 2015):

- $\sigma_{ij} = x_{ij} + 2/3(DL_j)$ for samples below LOD, and
- $\sigma_{ij} = 0.2x_{ij} + 2/3(DL_j)$; $DL_j < x_{ij} < 3DL_j$ and $\sigma_{ij} = 0.1x_{ij} + 2/3(DL_j)$; $x_{ij} > 3DL_j$ for detected values

where x_{ij} is the determined concentration for species j in the i^{th} sample and DL_j is the detection limit for species j .

A1.4.1.2 Limits of Detection and Uncertainty Reporting for Elements Determined by Ion Beam Analysis

For IBA, to determine the concentration of each element, the background is subtracted and peak areas fitted and calculated. The background occurs through energy loss, scattering and interactions of the ion beam as it passes through the filter material or from γ -rays produced in the target and scattered in the detector system (Cohen 1999). The peaks of elements in spectra that have interferences or backgrounds from other elements present in the air particulate matter, or filter matrix itself, will have higher LOD. The IBA was performed using a 3 MeV accelerator proton beam with standards (SrF₂, NaCl, Cr, Ni, SiO, KCl, Al) run before and after each analytical cycle. Spectral X-ray peak deconvolution was performed using GUPIX software (Maxwell et al. 1989, 1995). The number of pulses (counts) in each peak for a given element is used by the GUPIX software to calculate the concentration of that element. The background and neighbouring elements determine the statistical error and LOD. Note that GUPIX provides a specific statistical error (uncertainty) and LOD for each element in each particulate matter sample. The statistical uncertainty is calculated from the X-ray-peak fitting process (called the fit error) and is related to the square root of the peak area. The LOD for an element in each sample spectra is defined as three times the error (3σ) obtained for the background and overlap (but not the element's own area) in a 1 full-width-half-maximum region centred about the principal X-ray peak of the element. The summary statistics provided for elemental concentrations in each dataset are therefore averages of the individual uncertainty and LOD values.

Choice of filter material is an important consideration with respect to elements of interest, as is avoiding sources of contamination. The GNS Science IBA laboratory routinely runs filter blanks to correct for filter-derived analytical artefacts as part of their quality assurance and control procedures. Figure A1.7 shows the LODs typically achieved by PIXE for each element at the GNS Science IBA facility. All IBA elemental concentrations determined in this work were accompanied by their respective LODs. The use of elemental LODs is important in receptor modelling applications.

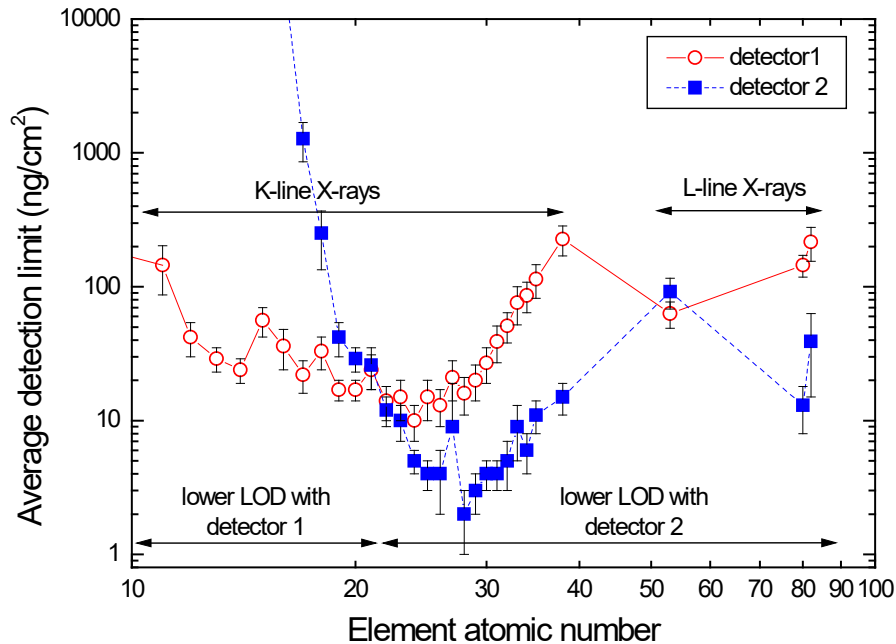


Figure A1.7 Elemental limits of detection for particle-induced X-ray emission routinely achieved at the GNS Science Ion Beam Analysis facility for air filters.

A1.5 Dataset Quality Assurance

Quality assurance of sample elemental datasets is vital so that any dubious samples, measurements and outliers are removed, as these will invariably affect the results of receptor modelling. In general, the larger the dataset used for receptor modelling, the more robust the analysis. The following sections describe the methodology used to check data integrity and provide a quality assurance process that ensured that the data being used in subsequent factor analysis were as robust as possible.

A1.5.1 Mass Reconstruction and Mass Closure

Once the sample analysis for the range of analytes has been carried out, it is important to check that total measured mass does not exceed gravimetric mass (Cohen 1999). Ideally, when elemental analysis and organic compound analysis has been undertaken on the same sample, one can reconstruct the mass using the following general equation for ambient samples as a first approximation (Cahill et al. 1990; Malm et al. 1994; Cohen 1999):

$$\text{Reconstructed mass} = [\text{Soil}] + [\text{OC}] + [\text{BC}] + [\text{Smoke}] + [\text{Sulphate}] + [\text{Sea salt}] \quad \text{Equation A1.4}$$

where:

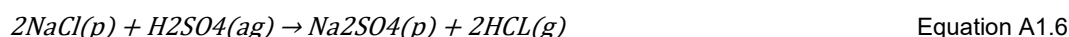
- $[\text{Soil}] = 2.20[\text{Al}] + 2.49[\text{Si}] + 1.63[\text{Ca}] + 2.42[\text{Fe}] + 1.94[\text{Ti}]$
- $[\text{OC}] = \Sigma[\text{Concentrations of organic compounds}]$

- [BC] = Concentration of black carbon (soot)
- [Smoke] = [K] – 0.6[Fe]
- [Sea salt] = 2.54[Na]
- [Sulphate] = 4.125[S]

The reconstructed mass (RCM) is based on the fact that the six composite variables, or ‘pseudo’ sources, given in Equation A1.4 are generally the major contributors to fine and coarse particle mass and are based on geochemical principles and constraints. The [Soil] factor contains elements predominantly found in crustal matter (Al, Si, Ca, Fe, Ti) and includes a multiplier to correct for oxygen content and an additional multiplier of 1.16 to correct for the fact that three major oxide contributors (MgO, K₂O, Na₂O), carbonate and bound water are excluded from the equation.

[BC] is the concentration of black carbon, measured in this case by light reflectance/absorbance. [Smoke] represents K not included as part of crustal matter and tends to be an indicator of biomass burning.

[Sea-salt] represents the marine aerosol contribution and assumes that the NaCl weight is 2.54 times the Na concentration. Na is used as it is well known that Cl can be volatilised from aerosol or from filters in the presence of acidic aerosol, particularly in the fine fraction via the following reactions (Lee et al. 1999):



Alternatively, where Cl loss is likely to be minimal, such as in the coarse fraction or for both size fractions near coastal locations and relatively clean air in the absence of acid aerosol, then the reciprocal calculation of [Sea-salt] = 1.65[Cl] can be substituted, particularly where Na concentrations are uncertain.

Most fine sulphate particles are the result of oxidation of SO₂ gas to sulphate particles in the atmosphere (Malm et al. 1994). It is assumed that sulphate is present in fully neutralised form as ammonium sulphate. [Sulphate] therefore represents the ammonium sulphate contribution to aerosol mass with the multiplicative factor of 4.125[S] to account for ammonium ion and oxygen mass (i.e. $(\text{NH}_4)_2\text{SO}_4 = ((14 + 4) \times 2 + 32 + (16 \times 4) / 32)$).

Additionally, the sulphate component not associated with sea-salt can be calculated (Cohen 1999) by:

$$\text{Non-sea-salt sulphate (NSS-Sulphate)} = 4.125 ([S_{\text{tot}}] - 0.0543[\text{Cl}]) \quad \text{Equation A1.7}$$

where the sulphur concentrations contributed by sea-salt are inferred from the chlorine concentrations, i.e. [S/Cl]_{sea-salt} = 0.0543, and the factor of 4.125 assumes that the sulphate has been fully neutralised and is generally present as (NH₄)₂SO₄ (Cahill et al. 1989; Malm et al. 1994; Cohen 1999).

The RCM and mass closure calculations using the pseudo-source and pseudo-element approach are a useful way to examine initial relationships in the data and how the measured mass of species in samples compares to gravimetric mass. Note that some scatter is possible because not all aerosols are necessarily measured and accounted for, such as all OC, ammonium species, nitrates and unbound water.

A1.5.1.1 Dataset Mass Reconstruction Summary for Auckland Particulate Matter Speciation Sites

Using the methodology outlined in Section A1.4.1, the following figures present the mass reconstruction results for PM₁₀ collected at the current Auckland Council particulate matter speciation monitoring sites.

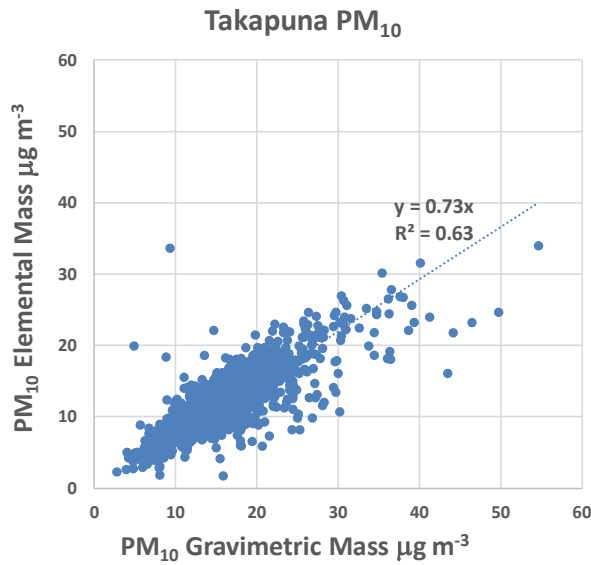


Figure A1.8 Plot of elemental mass reconstruction against gravimetric for Takapuna PM₁₀ mass.

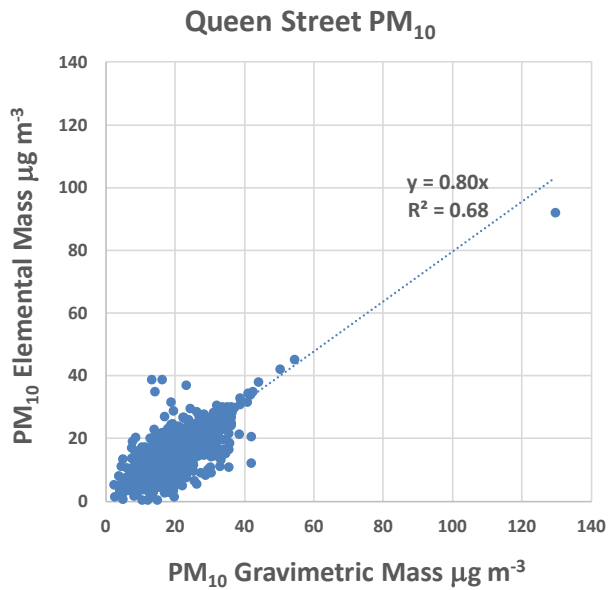


Figure A1.9 Plot of elemental mass reconstruction against gravimetric for Takapuna PM₁₀ mass.

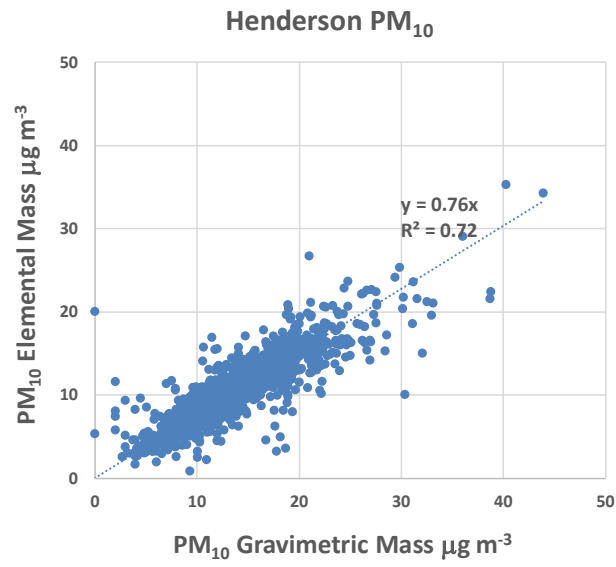


Figure A1.10 Plot of elemental mass reconstruction against gravimetric for Henderson PM₁₀ mass.



www.gns.cri.nz

Principal Location

1 Fairway Drive, Avalon
Lower Hutt 5010
PO Box 30368
Lower Hutt 5040
New Zealand
T +64-4-570 1444
F +64-4-570 4600

Other Locations

Dunedin Research Centre
764 Cumberland Street
Private Bag 1930
Dunedin 9054
New Zealand
T +64-3-477 4050
F +64-3-477 5232

Wairakei Research Centre
114 Karetoto Road
Private Bag 2000
Taupo 3352
New Zealand
T +64-7-374 8211
F +64-7-374 8199

National Isotope Centre
30 Gracefield Road
PO Box 30368
Lower Hutt 5040
New Zealand
T +64-4-570 1444
F +64-4-570 4657